Glueball Spectra in the Presence of a Magnetic Field.

Utrecht University

Utrecht University

Sandra Hollander

Supervisor:
Umut Gürsoy

February 11, 2021

Abstract

One of the interesting properties of QCD is the fact that the carriers of the strong force, gluons, are able to interact with themselves. This allows for the gluons to form bound states in the form of glueballs. To find out more about the properties of these glueballs, we study how their mass spectrum reacts to an external magnetic field in the case of strong interactions. For this, we use improved holographic QCD to construct a gravitational dual to pure Yang-Mills theory which is coupled to a constant external magnetic field. Surprisingly, we find that for increasing values of the magnetic field strength, the masses decrease. This is the opposite of effects known from Landau quantization, where a stronger external magnetic field heightens the mass spectra.

Contents

1 Introduction **3**

2 QCD **5**

3 AdS/CFT correspondence **8**

3.1 AdS/CFT 8

3.1.1 AdS space 8

3.2 Improved Holographic QCD 11

3.3 Confinement Conditions 15

3.4 Mass Spectrum 17

4 The Holographic Model **21**

4.1 Action and Equations of Motion 21

4.2 Ground State Solutions 25

4.3 Confinement Conditions 27

4.4 Boundary Conditions 29

4.4.1 IR Limit 29

4.4.2 UV Limit 36

4.5 Solving to the Equations of Motion 39

5 Mass Spectrum **44**

6 Conclusion **48**

Chapter 1

Introduction

In the 1950s technological developments enabled the use of high energy particle beams. This lead to the discovery of many particles with a short lifespan. As a result, there was a desperate need for a theory which could explain their existence. This came in the mid-1960s when Gell-Mann and Zweig, independently, suggested the *quark model* as an underlying model for these particles. They postulated that all the newly discovered particles are in fact bound states of small constistuents called quarks.[1]

In 1971 Gell-Mann and Fritzsch expanded on this theory. They came with a model of quarks where they assumed that the quarks have a new type of quantum number: color. The color group, consisting of three colors was assumed to have a $SU(3)$ symmetry. Later, it was found that they could interpret this color group as a gauge group. The gauge theory that came as a result is similar to quantum electrodynamics. Just like there is an electromagnetic force that binds two oppositely charged particles, there is also a force binding the quarks: the *strong force*. The carriers of this force, called gluons, are generated by the gauge bosons coming from this theory. Unlike photons however, gluons are also able to interact with themselves. [2]

The fact that gluons can interact with themselves, leads to interesting physics. The consequence of this fact we are going to focus on, is that gluons can form a bound state called *glueballs*. At present, there is still a lot unknown about these glueballs. This is because experimentally, they are difficult to detect as they mix with other hadrons. On the other hand, making theoretical calculations about glueballs proves to be difficult as well because you need to consider the strongly interacting regime of QCD.

Our main goal is to find out more about how these glueballs react to the presence of an external magnetic field. QCD is already known to be able to be influenced by the presence of an external magnetic field and there have already been many studies about this influence. In [3, 4, 5, 6] for example, the QCD phase diagrams under influences of a magnetic field, magnetic catalysis and Landau levels of quarks are studied.

What we want to find out, and is the main focus of this project, is to find out how the presence of an external magnetic field influences the spectrum of glueballs. For charged particles with weak couplings, the effect of a magnetic field on the spectrum is already known. This is described by Landau quantization. Here, the energy levels and the magnetic field strength B are related as follows [7]:

$$E_n = \hbar\omega_c \left(n + \frac{1}{2}\right) + \frac{p_z^2}{2m} \tag{1.1}$$

with,

$$\omega_c = \frac{qB}{mc} \tag{1.2}$$

Glueballs however don't carry color charge, and we consider a strongly interacting regime here, so it would be interesting to see if glueballs behave similarly or if we get a completely different response to a magnetic field.

To study the glueball spectra, we use improved holographic QCD (ihQCD) to construct a simplified model. It should be noted however, that only pure Yang-Mills theory is considered here, the quarks are left out of this model.

The rest of the thesis has the following structure: We start a qualitative review of QCD and its properties. Next, we discuss the AdS/CFT correspondence and the theory we will be using: improved holographic QCD (ihQCD). During the discussion of ihQCD, we will discuss the properties we want the model to have, such as quark confinement. Using this knowledge, we then construct a model in which the magnetic field is included. We start with a very general model and fix the parameters and boundary conditions such that we end up with a model in the ground state, with quantum confinement and where we can vary the magnetic field strength B. After this, we consider fluctuations around the gravitational background and extract the particle spectrum for various values of the magnetic field strength B.

Chapter 2

QCD

As mentioned in the introduction, quarks form the constituents of many particles. They are bound together through strong force, which is realised by the exchange of gluons. The dynamics of quarks and gluons are controlled by the following Lagrangian:

$$\mathcal{L} = -\frac{1}{4} F^{\alpha}_{\mu\nu} F^{\mu\nu}_{\alpha} + \bar{\Psi}_{\nu} \left(i\gamma^{\mu} D_{\mu} - m \right) \Psi^{\nu}. \tag{2.1}$$

Here, $F^{\alpha}_{\mu\nu}$ describes the gauge-field strength and is given by:

$$F^{\alpha}_{\mu\nu} = \partial_{\mu} A^{\alpha}_{\nu} - \partial_{\nu} A^{\alpha}_{\mu} + g f^{abc} A^{b}_{\mu} A^{c}_{\nu}, \tag{2.2}$$

where A_{μ} describes the gauge fields. Furthermore, the fields Ψ_{μ} denote the quark fields, the covariant derivative is given by:

$$D_{\mu} = \partial_{\mu} - igA^{\alpha}_{\mu} t^{\alpha} \tag{2.3}$$

and g denotes the coupling constant [8].

Despite this Lagrangian looking deceptively simple, there are difficulties when working with this theory. QCD is a theory with asymptotic freedom. This means the interactions between particles become asymptotically weaker as the energy scale increases. At high energies, the coupling constant is small, allowing the use of perturbative calculations. On the other hand for smaller energies, which are also the energy scales we are interested in, the coupling constant becomes too large to be able to use perturbative calculations effectively. This makes calculations very difficult to perform analytically.

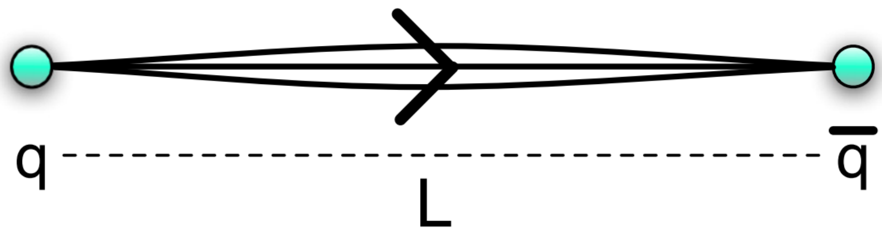

Figure 2.1: Linear confinement in QCD-like theories. Taken from [10]

Another property of QCD is color confinement. It is based on the idea that color charged particles cannot be separated. While there is no analytic proof, it can be qualitatively understood as the result of the interactions of gluons. In contrast to the electromagnetic force, where photons do not self-interact and the field lines spread out, the gluons which can self-interact, stay confined to a 'tube' between the quarks. At relatively large distances, the density of the gluons is constant [9]. As a result, the binding force between the quarks remains roughly constant and the potential takes the form:

$$V_{q\bar{q}}(L) = \sigma_0 L + \dots, \tag{2.4}$$

where L denotes the distance between the quarks. Because V increases linearly with increasing L, it would take an infinite amount of energy to separate the quarks and thus explains why singular color charged particles are not observed.

As mentioned before, when working at low enough energy scales, the coupling constant becomes too large and perturbative methods fail. Therefore, it becomes necessary to switch to non-perturbative methods. Lattice-QCD is the most well-established among these. Instead of a continuous space-time, a discrete lattice is considered here and all quarks and gluons can only exist on the lattice points. As a result, there is a minimum distance α, the distance between two neighbouring lattice points, between the quarks and gluons which cannot be breached. This removes the divergency in the ultraviolet section.

Another advantage of transcribing QCD onto a lattice is that it calculations

	$J^{PC} = 0^{++}$	$J^{PC} = 2^{++}$
n=0	1475 MeV	2150 MeV
n=1	2755 MeV	2880 MeV
n=2	3370 MeV	
n=3	3990 MeV	

Table 2.1: Spectra for glueballs with $J^{pc} = 0^{++}$ and $J^{pc} = 2^{++}$, taken from [12]

can be performed with methods analogous to well-known methods used in condensed matter theory. [11]. Through these calculations, the partition function and matrix elements of any operator between two hadronic states can be calculated numerically. Furthermore, the effective masses of glueballs can be determined by studying the propagator of these particles. This has been done in [12], for which the results are shown in Table 2.1.

There are disadvantages to lattice QCD, however. Besides the fact that calculations using lattice QCD are slow and resource intensive, in the calculation of real-time operators there are systemetic and statistical errors that can provide inaccurate results. [10]. Because of these reasons, there has been a demand for an alternative method. This demand has been realised when it was found out that through the AdS/CFT correspondence an alternative formulation for QCD can be made.

It should be noted, however, that this approach often makes use of a toy model of QCD, where only the properties of QCD thought to be relevant are included. For our research this is also the case. Here, we leave out the contribution of the quarks to the theory and only consider a pure Yang-Mills theory given by the Lagrangian:

$$\mathcal{L}_{YM} = -\frac{1}{4}\mathrm{Tr}(F^2). \tag{2.5}$$

As can be seen, only the part of $\mathcal{L}_{QCD}$ which describes the gluon-gluon interactions is included here.

Chapter 3

AdS/CFT correspondence

3.1 AdS/CFT

To understand AdS/CFT, it is important to understand the concept of duality. This refers to the fact that two concepts which are physically very different are the same on a mathematically deep level. By making use of the mathematical similarities, a dictionary can be created which maps properties of one side of the duality onto the other side.

AdS/CFT makes use of such a duality. It provides a link between quantum field theory on a flat four-dimensional spacetime and a gravitational theory in five dimensions. The AdS/CFT-correspondence is a realisation of the holographic principle, which states that in a gravitational theory, the number of degrees of freedom in a given volume V scales with the surface volume ∂V. As a result, the information on the surface volume encodes the information about the volume V.

In the case of AdS/CFT this principle is used to link the information of a quantum field theory on four-dimensional Minkowski spacetime onto a higher dimensional space which is locally Minkowski near the boundary. A five-dimensional spacetime satisfying this property and used in the AdS/CFT correspondence is the five-dimensional Anti-deSitter space.

3.1.1 AdS space

Anti-deSitter space describes a negatively curved spacetime which is maximally symmetric. It can be embedded into a Minkowski spacetime $(X^0, \ldots, X^{d+1})$

which has one extra dimension and is given by the metric:

$$ds^2 = -(dX^0)^2 + (dX^1)^2 + \cdots + (dX^d)^2 - (dX^{d+1})^2 \tag{3.1}$$

The embedding consists of a hypersurface which satisfies:

$$-(X^0)^2 + (X^1)^2 + \cdots + (X^d)^2 - (X^{d+1})^2 = -L^2, \tag{3.2}$$

where L denotes the radius of the anti-deSitter space. [13].

To see how AdS is locally similar to Minkowski space, consider the following coordinate transformation to the coordinates $(t, \vec{x}, r)$ with $t \in \mathbb{R}$, $\vec{x} = (x^1, \dots, x^{d-1}) \in \mathbb{R}^{d-1}$ and $r \in \mathbb{R}$:

$$\begin{aligned} X^0 &= \frac{L^2}{2r}\left(1 + \frac{r^2}{L^4}\left(\vec{x}^2 - t^2 + L^2\right)\right) \\ X^i &= \frac{rx^i}{L} \text{ for } i \in \{1, \dots, d-1\} \\ X^d &= \frac{L^2}{2r}\left(1 + \frac{r^2}{L^4}\left(\vec{x}^2 - t^2 - L^2\right)\right) \\ X^{d+1} &= \frac{rt}{L} \end{aligned} \tag{3.3}$$

Since only positive values of r are allowed, only half of the AdS space is described by these coordinates. However, to see how AdS_5 behaves locally, this suffices. The coordinates used here are also known as the Poincaré patch. With these coordinates, the metric now reads:

$$ds^2 = \frac{L^2}{r^2}dr^2 + \frac{r^2}{L^2}\left(-dt^2 + d\vec{x}^2\right) \tag{3.4}$$

For fixed values of r, we find that the metric reduces to a d-dimensional Minkowski spacetime $\mathbb{R}^{d-1,1}$. At the conformal boundary $r \to \infty$, we therefore find that AdS_{d+1} locally behaves as $\mathbb{R}^{d-1,1}$. In general, the quantum gravity theory of AdS/CFT lives on a manifold $AdS \times X$, where X denotes a compact space.

We will now look at a well-known example of AdS/CFT. This links $\mathcal{N} = 4$ Yang-Mills theory to a type IIB string theory which lives on a compactified $AdS_5 \times S^5$ space. The relation, also known as the Gubser-Klebanov-Polyakov-Witten relation and is given by:

$$\langle e^{\int d^dx\,\mathcal{J}(x)\mathcal{O}(x)}\rangle_{CFT} = \int \mathcal{D}\Phi e^{-S_{AdS}}\Big|_{\Phi(x,\partial AdS)=\mathcal{J}(x)}. \tag{3.5}$$

For the parameters of both sides of the duality, we have the following relations:

$$g_s \sim g_{YM}^2 \qquad Rl_s^2 \sim (g_{YM}^2 N_c)^{-1/2}. \tag{3.6}$$

Here, g_s denotes the coupling constant in the string theory, g_{YM} is the coupling constant of the gauge theory, RL_s^2 is the Ricci curvature of the background in terms of string units and N_c stands for the number of colors. In the limit

$$N_c \to \infty, \lambda \equiv g_{YM}^2 N_c \to \infty, \tag{3.7}$$

the coupling $g_s \to 1$ while Rl_s^2 becomes sufficiently small. As a result, at leading order in g_s, the theory on the AdS side of the duality reduces to semi-classical gravitational theory.

One final relation we need to establish between both sides of the duality is a relation between the operators in the Yang-Mills theory and the fields in the gravitational theory. For this we use the operator-field correspondence.

Consider an operator $\mathcal{O}(x)$ that is sourced by the field $\mathcal{J}(x)$. The dual for such an operator in the gravitational theory is given by a field $\Phi(x,r)$. Close to the boundary of the AdS-space, there are two independent solutions for this field. They scale with z^{Δ} and $z^{(d-\Delta)}$ respectively, where Δ is the scaling dimension given by $\Delta = \frac{d}{2} + \nu$, $\nu = \sqrt{m^2R^2 + \frac{d^2}{4}}$, with m describing the mass of bulk field and where d denotes the dimension of the string theory. We can therefore write $\Phi(x,r)$ as

$$\Phi(r,x) = A(x)r^{d-\Delta} + B(x)r^{\Delta} \tag{3.8}$$

near the boundary.
The functions $A(x)$ and $B(x)$ are related to properties of the operator $\mathcal{O}(x)$. Specifically, $A(x)$ corresponds with the source $\mathcal{J}(x)$ and $B(x)$ is related to the vacuum expectation value $\langle\mathcal{O}(x)\rangle$ by $B(x) = \frac{\mathcal{O}(x)}{2\nu}$. This gives:

$$\Phi(r,x) = \mathcal{J}(x)r^{d-\Delta} + \frac{\langle\mathcal{O}(x)\rangle}{2\nu}r^{\Delta}, \tag{3.9}$$

From the behaviour of $\Phi(x,r)$ near the boundary, we can therefore already extract important information about the properties of the operator. So is

YM	**gravity**
energy-momentum field tensor T_{ab}	metric field g_{ab}
scalar operator $\mathcal{O}_b$	scalar field ϕ
fermionic operator $\mathcal{O}_f$	Dirac field ψ

Table 3.1: Examples of operators and their corresponding fields.

the leading term of $\Phi(x, r)$ directly related to the source of the operator, while the vacuum expecation value of the operator can be extracted from the subleading term.

By making use of these relations, we can create a dictionary between the operators and fields. Examples of related operators and fields can be found in Table 3.1.

Besides the expectation values for operators, two-point correlators can also be extracted from the field-operator relation. On the field theory side of the relation, we find that the two-point function can be derived by taking the derivative with respect to $\mathcal{J}(x)$ twice and setting $\mathcal{J}$ to zero. To perform the same steps on the gravity side, one first has to determine the classical solution $\Phi(r, x)$ in terms of $\mathcal{J}(x)$ with the boundary condition $\phi(0, x) = \mathcal{J}(x)$. By substituting this solution in S_{AdS}, the right-hand side of Eq. 3.5 is now written in terms of $\mathcal{J}(x)$. Now, after taking the derivative with respect to $\mathcal{J}(x)$ twice and setting $\mathcal{J}(x)$ to zero, the two-point function is determined on the string side of the duality.

3.2 Improved Holographic QCD

With the basics of AdS/CFT explained, we now discuss how this correspondence can be used to construct a dual theory to QCD. For this, we briefly look at different approaches that have already been tried to find this relation and discuss their advantages and disadvantages.

Top-down approach: In the top-down approach you start with a certain D-brane configuration and take the *decoupling limit* as described in [14]. This way the D-brane configuration gets replaced by a gravitational background with various form fields. While this correspondence gives a precise relation between the D-branes and the QFT, it not only results in a theory different than QCD or pure Yang-Mills theory but also has an additional sector in the Hilbert space spanned by infinite many operators. While the second problem is also present in the $\mathcal{N} = 4$ SYM theory, the operators there are in direct correspondence with higher conformal dimension. In QCD however, this is not the case, which provides many difficulties. [15], [14]. As a result, a different approach was considered.

Bottom-up approach: In the bottom-up approach, the goal of giving a precise dual to QCD is given up. Instead, a theory is constructed which only captures the infrared dynamics of the operators in the QCD theory.

In early theories a *hard-wall* model was considered. Here, to ensure only the infrared dynamics are encaptured, a strict cut-off in the gravitational theory is introduced somewhere deep in the interior. However, these models gave unrealistic results such as $m_n^2 \propto n^2$ for large n [16], [17]. To overcome these problems, the hard-wall was made less strict by introducing, instead of a cut-off, a dilaton to the AdS_5 gravitational theory whose profile was chosen by hand to obtain realistic features. However, in this new *soft-wall* model, there were still unrealistic features present in the glue sector and in the thermodynamics of the theory [18].

Improved holographic QCD: In improved holographic QCD, instead of choosing the background by hand, it is obtained by minimizing the action for gravity coupled to a scalar field. For this theory only the parts of QCD are considered which involve the so-called *low-lying* operators. Furthermore, the gravitational dual we wish to construct should be a dual to a $SU(N_c)$ gauge theory in the large N_c limit. The three relevant operators for this theory are the stress tensor $T_{\mu\nu}$, the scalar glueball operator $\mathrm{tr}F^2$ and the axionic glueball operator $\mathrm{tr}F \wedge F$. The last operator, however, is shown to scale with $1/N_c$ and can thus be treated as a perturbation in the limit $N_c \to \infty$. For the remaining two operators it is propsed that $T_{\mu\nu}$ should be dual to $g_{\mu\nu}$ and $\mathrm{tr}F^2$ should be dual to the dilaton Φ in the gravitational theory.

As a starting point for the gravity side of the duality, consider the following Einstein-Dilaton action:

$$S = M_p^3 N_c^2 \int d^5x \sqrt{-g} \left(R - \frac{4}{3}(\partial\Phi)^2 + V(\Phi) \right) + S_{GH} + \mathrm{S}_{ct} \tag{3.10}$$

Here, M_p represents Plank energy scale, N_c denotes the number of colors and S_{GH} refers to the Gibson-Hawking term given by:

$$S_{GH} = 2M_p^3 \int_{\partial M} d^4x\sqrt{h}K, \tag{3.11}$$

with

$$\begin{aligned} K_{\mu\nu} = -\nabla_\mu n_\nu = \frac{1}{2}n^\rho \partial_\rho h_{\mu\nu} \\ K = h^{ab}K_{ab}, \end{aligned} \tag{3.12}$$

where h_{ab} refers to the induced metric and n^μ is the unit normal to the boundary. Both the dilaton and the metric fields are assumed to be dependent on a holographic coordinate u which runs from the boundary $u \to -\infty$ to the origin at an interior point $u = u_0$. In the vacuum state, with vanishing temperature, the boundary of this theory should have $SO(3,1)$ symmetry. This gives us the following ansatz for the metric:

$$ds^2 = du^2 + e^{2A(u)}\eta_{\mu\nu}dx^\mu dx^\nu \tag{3.13}$$

From the action and metric described above, the equations of motion for $A(r)$ and $\Phi(r)$ can now derived and are given by:

$$\begin{aligned} A'' = \frac{-4}{9}(\Phi')^2 \\ 3A'' + 12(A')^2 = V(\Phi). \end{aligned} \tag{3.14}$$

By choosing the right boundary conditions for $A(r)$, $\Phi(r)$ and an expression for the potential $V(\Phi)$, the fields $A(r)$ and $\Phi(r)$ can be fully determined from which one can, eventually, derive the glueball spectra as we will show later on.

One important concern to consider for this approach, however, is that we consider the limit $N_c \to \infty$, while we know that in QCD, the number of colors is given by $N_c = 3$. Luckily, lattice calculations show, that after normalization, various observables of QCD remain the same for varying values of N_c [19]. Moreover, the results for ihQCD, are also consistent with these results [10]. An example of this fact is shown in Fig. 3.1, where the trace of the EM-tensor is calculated for different values of N_c.

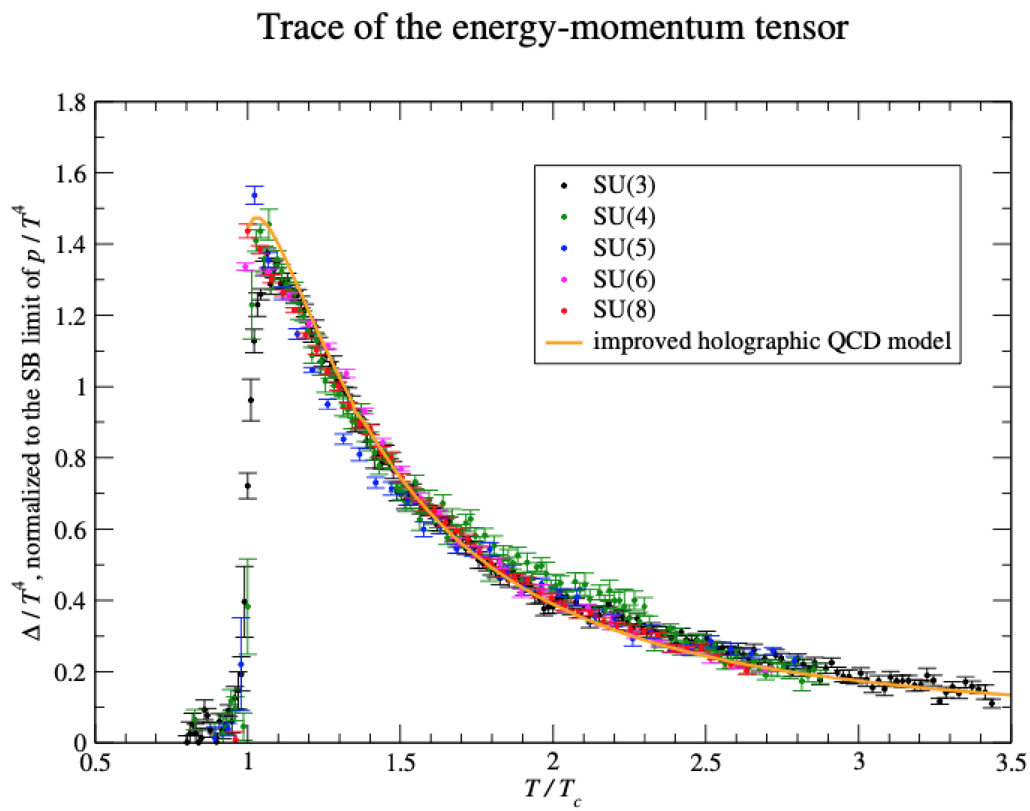

Figure 3.1: Trace of the energy momentum tensor for various values of N_c. Taken from [10]

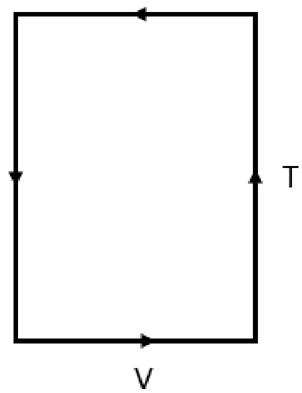

Figure 3.2: Schematic picture of a Wilson loop $\mathcal{C}$.

3.3 Confinement Conditions

For the model above, we still need to ensure that there is quark confinement present. To determine the conditions for this, we closely follow the discussion of [20], where through the use of Wilson loops, the behaviour of the quark-antiquark potential $E(L)$ is determined.

Firstly, we first study the expectation value of a Wilson loop on both sides of the duality as motivated in [21]. There, it is stated that for a rectagular Wilson loop $\mathcal{C}$ with sides T and L (as shown in Fig. 3.2), the expectation of the Wilson loop in the Yang-Mills theory is given by:

$$\langle W(\mathcal{C})\rangle = A(L)e^{-TE(L)}. \tag{3.15}$$

On the string theory side of the duality, the expectation value of the Wilson loop is proposed to be:

$$\langle W(\mathcal{C})\rangle \sim e^{-S}, \tag{3.16}$$

where S describes the area of the world-sheet for which boundary coincides with the Wilson Loop $\mathcal{C}$ in the UV limit (which denotes the region where $u \to -\infty$). This gives the relation:

$$S_{NG}[X_\mu^{\min}(\sigma,\tau)] = TE(L), \tag{3.17}$$

where S denotes the Nambu-Goto action.

Direct calculation shows that for a general 5D metric of the form:

$$ds^2 dx^\mu dx^\nu = g_{rr} dr^2 - g_{00} dt^2 + g_{\parallel} d\vec{x}_{\parallel}^2 + g_{\perp} d\vec{x}_{\perp}^2, \tag{3.18}$$

where $x_\perp$ describe the coordinates of the space transverse to the Wilson Loop, $S_{NG}[X_\mu^{\min}(\sigma,\tau)]$ equals:

$$\begin{aligned} S &= \int d\sigma d\tau \sqrt{\det\left[\left(\partial_\alpha X^M\right)\left(\partial_\beta X^N\right) g_{MN}\right]} \\ &= T \int dx \sqrt{\det\left[g_{00}(s(x)) g_{\parallel}(s(x)) + g_{00}(s(x)) g_{ss}(s(x)) \left(\partial_x s\right)^2\right]} \\ &= T \int dx \sqrt{\det\left[f^2(s(x)) + g^2(s(x)) \left(\partial_x s\right)^2\right]}, \end{aligned} \tag{3.19}$$

with

$$\begin{aligned} f^2(s(x)) &\equiv g_{00}(s(x)) g_{\parallel}(s(x)) \\ g^2(s(x)) &\equiv g_{00}(s(x)) g_{ss}(s(x)). \end{aligned} \tag{3.20}$$

Therefore, we find that E is given by:

$$E = \int dx \sqrt{\det\left[f^2(s(x)) + g^2(s(x)) \left(\partial_x s\right)^2\right]}. \tag{3.21}$$

From the Lagrangian $\mathcal{L}(s, s') = \sqrt{\det\left[f^2(s) + g^2(s)(s')^2\right]}$, one can calculate the differential equation for a geodesic line which minimizes this action. This is given by:

$$\frac{ds}{dx} = \pm \frac{f(s)}{g(s)} \frac{\sqrt{f^2(s) - f^2(s_0)}}{f(s_0)}, \tag{3.22}$$

where $s_0 = s(0)$ which satisfies $s'(0) = 0$. The distance between the quark and anti-quark can now be calculated as:

$$L = \int dx = \int \left(\frac{ds}{dx}\right)^{-1} ds = 2 \int_{s_0}^{s_1} ds \frac{g(s)}{f(s)} \frac{1}{\sqrt{f^2(s)/f^2(s_0) - 1}}. \tag{3.23}$$

In these terms, the quark-antiquark potential E can be rewritten as:

$$E(L) = f(s_0) L + 2 \int_{s_0}^{s_1} ds \, \frac{g(s)}{f(s)} \sqrt{f^2(s) - f^2(s_0)}. \tag{3.24}$$

For large L, the second term becomes sub-leading and the quark anti-quark potential behaves like $E(L) = \sigma L$, with σ a constant. This is what we want for confinement, so we study the conditions for $L \to \infty$.

To find out how this is achieved for the metric given by Eq. 3.13, we first transform to conformal coordinates (where the coordinate r is related to u by $dr = \exp(-A)du$) and work in the string frame (which is given by $(g_S)_{\mu\nu} = e^{4\phi/(D-2)} g_{\mu\nu}$[22] where D describes the dimension of the string theory). The metric is then given by:

$$ds^2 = e^{2A_s(r)} \left(dr^2 + \eta_{\mu\nu} dx^\mu dx^\nu \right). \tag{3.25}$$

In turn, we find that $f(r)$ and $g(r)$ are given by:

$$\begin{aligned} f^2(r) &= -\exp(4A_s(r)) \\ g^2(r) &= -\exp(4A_s(r)) \end{aligned} \tag{3.26}$$

Therefore,

$$L = 2\int_0^{r_F} dr \frac{1}{\sqrt{\exp(2A_s(r) - 2A_s(r_0)) - 1}} \tag{3.27}$$

If we Taylor expand the exponential around r_F, we find that:

$$L = 2\int_0^{r_F} dr \frac{1}{\sqrt{4(A_s'(r) - A'(r_F)) + \mathcal{O}(r - r_F)^2}}. \tag{3.28}$$

For $L \to \infty$ to be satisfied, A_s should therefore have a minimum and we can conclude that the conditions of quark confinement correspond with the condition that there exists a minimum in $A_s(r)$. In [20], it is shown that this condition is satisfied if the potential $V(\phi)$ scales with $e^{4\Phi/3}$ in the limit $u \to u_0$. Furthermore, $A(r)$ and $\Phi(r)$ should satisfy $\frac{d\phi}{3dA} = -\frac{1}{2}$ in this limit.

For the boundary conditions for $u \to -\infty$ on the other hand, one can derive an expression for $A(r)$ from the fact that the metric should resemble AdS_5. Furthermore, the behaviour of $\phi(r)$ and $V(\phi)$ in this limit can be derived from the perturbative beta-function of the $SU(N_c)$ gauge theory.

After choosing the boundary conditions such that is all satisfied, the fields $A(r)$ and $\Phi(r)$ can be numerically solved.

3.4 Mass Spectrum

With all the relevant fields determined, all that is left is the extraction of the glueball spectrum from this information. For this, finite energy fluctuations are considered around the gravitational background. These fluctuations should be normalizable near the boundary $u \to -\infty$ and at the origin $u = u_0$.

For the rest of this section, we consider conformal coordinates. The boundary and origin are here given by $r = 0$ and $r \to \infty$ respectively. Assuming the fluctuations are diffeomorphism invariant, the quadratic part of the action describing them is given by:

$$S[\xi] = \int drd^4x \, e^{2B(r)} \left((\partial_r \xi)^2 + (\partial_i \xi)^2 + M^2 \xi^2 \right). \tag{3.29}$$

After writing $\xi(x, r) = \xi(r)\xi^{(4)}(x)$, we are interested in the mass eigenstates $\Box\xi = m^2\xi$. Varying the action with respect to ξ gives:

$$\xi''(r) + 2B'(r)\xi'(r) + m^2\xi - M^2\xi = 0. \tag{3.30}$$

For 2^{++} glueballs, $B(r)$ and M^2 are given by $B(r) = 3/2A(r)$, $M^2(r) = 0$. The other glueballs we consider, 0^{++} glueballs, satisfy $B(r) = 3/2A(r) + \log|X|$,$M^2 = 0$ [20, 23].

As mentioned before, the fields describing these fluctuations should be normalizable near the boundary $r \to 0$ as well as when $r \to \infty$. Near the boundary, we find that $A(r) \to -log(r)$ and $X'(r) \to 0$. Therefore, the equation of motion is given by

$$\xi''(r) - \frac{3}{r}\xi'(r) + m^2\xi(r) = 0 \tag{3.31}$$

in this region. This is solved by:

$$\xi(r) = c_1 r^2 J_2(mr) + c_2 r^2 Y_2(mr),$$

where $J_2(r)$ denotes the Bessel function of first kind and $Y_2(r)$ denotes the Bessel function of second kind. As $r \to 0$, $J_2(r) \propto r^2$ and $Y_2(r) \propto r^{-2}$. Therefore, $\xi(r)$ behaves like:

$$\xi(r) = c_1 d_1 r^4 + c_2 d_2,$$

in the limit $r \to 0$, where d_1, d_2 are constants depending om m.

To make sure the energy of the fluctuation ξ is finite, we rewrite Eq. 3.30 such that it resembles a Schrödinger equation. After defining the potential

$$V_s(r) = B''(r) + B'(r)^2 \tag{3.32}$$

and writing $\xi(r)$ as

$$\xi = \psi(r)e^{-B(r)}, \tag{3.33}$$

we find that Eq. 3.30 now reads

$$-\psi''(r) + V_s(r)\psi(r) = m^2\psi(r). \tag{3.34}$$

In this form, we can now easily see that for the energy of the fluctuation ξ to be finite, the square-integrability condition in the Schrödinger equation should be satisfied. In other words, we must have:

$$\int |\psi(r)|^2 < \infty,$$

where $\xi(r) = e^{-B(r)}\psi(r)$.

As $r \to 0$, we find that $\psi(r) \to \xi(r)r^{-3/2} = c_1 r^{5/2} + c_2 r^{-3/2}$. Since the second term has a negative power of r, normalizability near the boundary $r = 0$ demands $c_2 = 0$. Therefore, $\xi(r) \propto r^4$ as $r \to 0$. Furthermore, as Eq. 3.30 is linear in ξ, the proportionality constant in $\xi(r) \propto r^4$ only affects the scale of ξ, but has no effects on normalizability. We can therefore choose this constant to equal one and have $\xi(r) = r^4$ near the boundary.

With the behaviour of ξ near the boundary determined, we still need to make sure that the energy fluctuation is finite as $r \to \infty$. This is exactly the case for the values of m^2 at which an extra node appears in the wave function $\psi(r)$. By varying the parameter m^2 until such an extra node appears, the masses are determined. Afterwards, the masses are rescaled such that the lowest lying masses from this calculation correspond with the ones obtained from the lattice calculations in [12]. This approach has already been done in [20] for which the results are shown in Table 3.2. As can be seen, there is a good match between both approaches.

J^{PC}	0^{++} (Lattice)	0^{++}(ihQCD)	$^{++}$ (Lattice)	2^{++} (ihQCD)
n=0	1475 MeV	1475 MeV	2150 MeV	2055 MeV
n=1	2755 MeV	2753 MeV	2880 MeV	2991 MeV
n=2	3370 MeV	3561 MeV		
n=3	3990 MeV	4253 MeV		

Table 3.2: Spectra for glueballs with $J^{pc} = 0^{++}$ and $J^{pc} = 2^{++}$ from both the lattice-QCD and ihQCD calculations, taken from [20, 12].

Chapter 4

The Holographic Model

4.1 Action and Equations of Motion

With a basic understanding of the isotropic scenario of improved holographic QCD, we now introduce an external magnetic field to the theory. This is done by adding a non-minimal coupling between the scalar dilaton and the electromagnetic field tensor described by $F_{\mu\nu} = \partial_\mu A_\nu - \partial_\nu A_\mu$. The action is now given by:

$$S = -\frac{1}{16\pi G}\int d^5x\sqrt{-g}\Big(R - \frac{4}{3}(\nabla\Phi)^2 - V(\Phi) - Z(\Phi)F_{\mu\nu}F^{\mu\nu}\Big). \tag{4.1}$$

We only consider the influence of magnetic fields. Specifically, one with a constant magnetic field strength B pointing in the $\vec{x}_3$-direction. The magnetic vector potential A_μ corresponding to this is given by:

$$A_\mu = (0, -yB/2, xB/2, 0, 0). \tag{4.2}$$

We also need to take the fact into account that with an external magnetic field pointing in the $\vec{x}_3$-direction, we cannot assume anymore that the space is spherically symmetric. Therefore, we modify the metric by introducing an factor $\exp(2W(r))$ to break the isotropy. Furthermore, to introduce a finite temperature, we make this metric similar to a black-hole metric by including a blackening factor $f(u)$. Later on, we derive the conditions of $f(u)$ for which this model is in the ground state. As we will show, multiplying the blackening factor with $\exp(2W)$ ensures that the ground state exactly corresponds with $f(r) = 1$. As this simplifies the calculations, this is also what we choose here for the metric. Therefore, we now have:

$$ds^2 = \frac{du^2}{f(u)e^{2W(u)}} + e^{2A(u)}(-dt^2 f(u)e^{2W(u)} + e^{2W(u)}dx_3^2 + dR_2^2). \tag{4.3}$$

To make the calculations simpler, we introduce a new function g which satisfies $f = \exp(g)$. Direct calculation gives the following Einstein equations:

$$A'' - A'W' - \frac{1}{3}g'W' - \frac{2}{3}W'^2 + \frac{4}{9}\phi'^2 + \frac{2}{3}B^2 Ze^{-4A-g-2W} = 0 \tag{4.4}$$

$$g'' + g'\left(4A' + 3W' + g'\right) = 0 \tag{4.5}$$

$$4A'W' - 2B^2 Ze^{-4A-g-2W} + g'W' + W'' + 3\left(W'\right)^2 = 0 \tag{4.6}$$

The fields A, W, g have a linear constrain:

$$\begin{aligned} 3A'g' + 12A'W' + 12\left(A'\right)^2 + 2B^2 Ze^{-4A-g-2W} + g'W' \\ + Ve^{-g-2W} + 2\left(W'\right)^2 - \frac{4\left(\phi'\right)^2}{3} = 0. \end{aligned} \tag{4.7}$$

And the dilaton equation of motion is given by:

$$4A'\phi' - \frac{3}{4}B^2 Z'e^{-4A-g-2W} + g'\phi' - \frac{3}{8}e^{-g-2W}V' + 3W'\phi' + \phi'' = 0. \tag{4.8}$$

There is still some freedom left in the solutions to these equations. A closer look shows that they are invariant under the following transformations:

$$\begin{gathered} u \to u + a \\ u \to e^{b/2}u, g \to g + b \\ g \to g + c, W \to W - \frac{c}{2}. \end{gathered} \tag{4.9}$$

To remove this ambiguity and to simplify the equations to first order differential equations, we introduce the following scalars:

$$X = \frac{\phi'}{3A'} \tag{4.10}$$

$$Y = \frac{g'}{4A'} \tag{4.11}$$

$$U = \frac{W'}{A'} \tag{4.12}$$

$$H = \frac{1}{A'} e^{-2A-W-g/2}. \tag{4.13}$$

As can be easily checked, these scalars are invariant under the transformations given in Eq. 4.9. The equations of motion can be rewritten in terms of these scalars by dividing through $A'(r)^2$ and rearranging the terms. For example, for $X(\phi)$ we can derive the following relation:

$$\begin{aligned} \frac{dX}{d\phi} = \frac{d\left(\frac{\phi'(r)}{3A'(r)}\right)}{dr}\frac{dr}{d\phi} &= \left(\frac{\phi''(r)}{3A'(r)} - \frac{\phi'(r)A''(r)}{3A'(r)^2}\right)\frac{1}{\phi'(r)} \\ &= \frac{1}{3X}\left(\frac{\phi''(r)}{3A'(r)^2} - X\frac{A''(r)}{A'(r)^2}\right) \end{aligned} \tag{4.14}$$

Using the equations of motion, the terms $\frac{\phi''(r)}{A'(r)^2}$ and $\frac{A''(r)}{A'(r)^2}$ can be rewritten in terms of the scalars and the functions $V(\phi)$ and $Z(\phi)$. This leaves an expression for $\frac{dX}{d\phi}$ which fully consists of X, Y, U and H and the functions $V(\phi)$, $Z(\phi)$. After following this procedure for X, Y, U and H we get the following expressions:

$$\begin{aligned} \frac{dX}{d\Phi} = -\frac{4}{3}\left(1 + \frac{3}{8X}\frac{d\log V}{d\Phi}\right)\left(1 + \frac{U^2}{6} + \frac{UY}{3} + U - X^2 + Y - \frac{B^2H^2Z}{6}\right) \\ + \frac{B^2H^2Z}{12X}\left(\frac{d\log Z}{d\Phi} - 2\frac{d\log V}{d\Phi}\right) \end{aligned} \tag{4.15}$$

$$\frac{dY}{d\Phi} = -\frac{4Y}{3X}\left(1 + \frac{U^2}{6} + \frac{UY}{3} + U - X^2 + Y - \frac{B^2H^2Z}{6}\right) \tag{4.16}$$

$$\frac{dU}{d\Phi} = -\frac{4U}{3X}\left(1 + \frac{U^2}{6} + \frac{UY}{3} + U - X^2 + Y - \frac{B^2H^2Z}{6}\left(1 + \frac{3}{U}\right)\right) \tag{4.17}$$

$$\frac{dH}{d\Phi} = -\frac{2H}{3X}\left(1 + \frac{U^2}{3} + \frac{2UY}{3} + U - 2X^2 + Y - \frac{B^2H^2Z}{3}\right). \tag{4.18}$$

Boundary conditions

With the equations of motion for the scalars determined, all that is left is to find proper boundary conditions. For this, we take a look at their behaviour near the event horizon. We know that at the event horizon, $f(u)$ must satisfy $f(u) = \exp(g(u)) = 0$. As a result, we find that according to Eq. [4.11,4.13], $Y = \frac{g'}{4A'} = \frac{f'}{4fA'}$ and $H = \frac{1}{A'}\exp(-2A - W - g/2) =$

$\frac{1}{A'\sqrt{f}}\exp(-2A-W)$ diverge. We do not, however expect the scalars X and U to diverge near the horizon. To make sure this does not happen, we expand the scalars near the horizon in terms of ϕ and ensure that the equations of motion remain consistent here.

To find out how Y behaves with respect to ϕ in this region, we perform a Taylor expansion of $f(u), \Phi(u)$ near the horizon u_h. This gives:

$$f(u) = f'(u_h)(u-u_h) + \mathcal{O}\left((u-u_h)^2\right)$$

$$\phi(u) = \phi_h + \phi'(u_h)(u-u_h) + \mathcal{O}\left((u-u_h)^2\right),$$

where $\phi_h \equiv \phi(u_h)$. This allows us to write $Y(u)$ as

$$Y = \frac{1}{4}\frac{f'(u_h) + \mathcal{O}(u-u_h)}{\left(f'(u_h)(u-u_h) + \mathcal{O}\left((u-u_h)^2\right)\right)A'(u)}$$

in this limit. Using the expansion of ϕ, we can write $u-u_h$ as:

$$u - u_h = \frac{\phi-\phi_h}{\phi'_h} + \mathcal{O}\left((\phi-\phi_h)^2\right).$$

Substituting this expression in $Y(u)$ then gives

$$Y = \frac{1}{4}\frac{f'(u_h) + \mathcal{O}(\phi-\phi_h)}{\left(f'(u_h)\frac{(\phi-\phi_h)}{\phi'(u_h)} + \mathcal{O}\left((\phi-\phi_h)^2\right)\right)\left(A'(u_h) + \mathcal{O}(\phi-\phi_h)\right)}$$

$$= \frac{1}{4}\frac{f'(u_h)}{f'(u_h)\frac{(\phi-\phi_h)}{\phi'(u_h)}A'(u_h)} = \frac{1}{4}\frac{\phi'(u_h)}{(\phi-\phi_h)A'(u_h)} = \frac{3}{4}\frac{X_h}{\phi-\phi_h}.$$

Because X is finite near the horizon, we find that $Y(\phi)$ behaves like $Y \sim \frac{1}{\phi-\phi_h}$ as $\phi \to \phi_h$. Furthermore, assuming that $A'(u), A(u), W(u)$ do not diverge as $u \to u_h$, we find that $H \sim \frac{1}{\sqrt{f}} \sim \frac{1}{\sqrt{\Phi-\Phi_h}}$.

As a result, we choose the following expansions for the scalars in this limit:

$$X = X_h + X_1(\phi-\phi_h) + \mathcal{O}\left((\phi-\phi^h)^2\right) \tag{4.19}$$

$$Y = \frac{Y_h}{\phi-\phi_h} + Y_1 + \mathcal{O}\left(\phi-\phi^h\right) \tag{4.20}$$

$$U = U_h + U_1(\phi-\phi_h) + \mathcal{O}\left((\phi-\phi^h)^2\right) \tag{4.21}$$

$$H^2 = \frac{H_h^2}{\phi - \phi_h} + H_1^2 + \mathcal{O}\left(\phi - \phi^h\right). \tag{4.22}$$

By substituting these expansions in Eqs. [4.15-4.18] we find that X_h, Y_h, U_h and H_h^2 satisfy the following relations:

$$\begin{aligned} X_H &= \lim_{\phi \to \phi_H} \left(-\frac{3}{8} \frac{d \log V}{d\phi} + \frac{U_H}{8} \left(\frac{d \log Z}{d\phi} - 2 \frac{d \log V}{d\phi} \right) \right) \\ Y_H &= \frac{3X_H}{4} \\ B^2 H_H^2 Z_H &= 2U_H Y_H. \end{aligned} \tag{4.23}$$

This leaves the value of U_h undetermined. To be certain U_h is not fixed by second order conditions, we also expand Equations [4.15-4.18] up to second order in ϕ. This fixes X_1, Y_1, U_1 and H_1 as:

$$\begin{aligned} X_1 &= \frac{U_H}{16} \left(\left.\frac{d^2 \log Z}{d\phi^2}\right|_{\phi_H} - 2 \left.\frac{d^2 \log V}{d\phi^2}\right|_{\phi_H} + \frac{2U_1}{U_H} \left(\left.\frac{d \log Z}{d\phi}\right|_{\phi_H} - 2 \left.\frac{d \log V}{d\phi}\right|_{\phi_H} \right) \right) - \frac{3}{16} \left.\frac{d^2 \log V}{d\phi^2}\right|_{\phi_H} \\ Y_1 &= \frac{3}{8} X_1 - \frac{3}{2} \frac{1}{(3 - U_H)} \left(1 - \frac{U_H^2}{6} + \frac{2U_H}{3} + \frac{U_1 X_H}{4} - X_H^2 - \frac{1}{4} U_H X_H \left.\frac{d \log Z}{d\phi}\right|_{\phi_H} \right) \\ U_1 &= \frac{1}{2} \left(\frac{1 + U_H}{3} \right) U_H \left.\frac{d \log Z}{d\phi}\right|_{\phi_H} - \frac{2U_H}{3X_H} \left(1 + \frac{2U_H}{3} - 2X_H^2 \right) \\ B^2 H_1^2 Z_H &= 2U_H Y_1 - \frac{U_H}{3 - U_H} \left(U_H^2 + \frac{3}{2} X_H \left(U_1 - 4X_H - U_H \left.\frac{d \log Z}{d\phi}\right|_{\phi_H} \right) \right), \end{aligned} \tag{4.24}$$

but leaves U_H invariant. In summary, we find that X_H converges to a value depending on $\frac{d \log V}{d\phi}$, $\frac{d \log Z}{d\phi}$ and U_H. Y diverges as $\frac{Y_H}{\phi - \phi_h}$ with Y_H given by $Y_H = \frac{3X_H}{4}$. $B^2 H^2 Z(\phi)$ behaves like $2UY$ near the horizon and U converges to a value U_H that is yet to be determined.

4.2 Ground State Solutions

For our research, we are interested in the glueball spectra in the ground state. To make sure we are working in the ground state in our model, we must set the entropy $S = 0$. The entropy is given by the area of the horizon divided by 4 times the gravitational constant. For the metric given in Eq. 4.3, this is given by:

$$S = \frac{\exp(3A_h + W_h)}{4G}, \tag{4.25}$$

where A_h and W_h are the values of A and W at the event horizon.

Furthermore, the temperature of the solution is obtained by requiring the absence of a conical singularity in the Euclidean solution at the event horizon. This fixes the temperature as:

$$T = -\frac{1}{4\pi}\frac{d\,(f\exp(2W))}{dr}\bigg|_{r=r_h} = -\frac{1}{4\pi}\frac{d\,(f\exp(2W))}{du}\exp(-A)\bigg|_{u=u_h} \tag{4.26}$$

The equation of motion Eq. 4.5 can be rewritten as:

$$(g'\exp(4A + 3W + g))' = 0 \tag{4.27}$$

Therefore, we must have

$$\begin{gathered}(g'\exp(4A + 3W + g)) = f'\exp(4A + 3W) = C\\ f' = C\exp(-4A - 3W)\\ f = f_b + C\int_{-\infty}^{u_h}\exp(-4A - 3W),\end{gathered} \tag{4.28}$$

where f_b gives the value of f as $u \to -\infty$. Since our model resembles AdS_5 at the boundary $u \to -\infty$, we must have $f_b = 0$. Furthermore, we require $f(u_h) = 0$.

We can now obtain the value of C by combining Eqs. 4.25,4.26 and 4.28 and using the fact that $f(u_h) = 0$. This gives:

$$C = -16\pi GTS. \tag{4.29}$$

Therefore, in the ground state where $S = 0$, we find that $C = 0$ and thus that f is constant and equal to 1. As a consequence, we find that $Y = 0$. Since U is finite at the horizon, and $B^2H^2Z(\phi)$ behaves as $B^2H^2Z(\phi) \sim 2UY$ near the horizon we conclude that $B^2H^2Z \to 0$ as $\phi \to \phi_h$. This does not assure that $B^2H^2Z(\phi)$ equals 0 for all u, however. For now though, to simplify the equations, we consider the case where $B^2H^2Z(\phi)$ is negligible compared to the other terms in Equations [4.15-4.18]. In this case, the scalar equations of motion reduce to:

$$\frac{dX}{d\Phi} = -\frac{4}{3}\left(1 + \frac{3}{8X}\frac{d\log V}{d\Phi}\right)\left(1 + U + \frac{U^2}{6} - X^2\right) \tag{4.30}$$

$$\frac{dU}{d\Phi} = -\frac{4U}{3X}\left(1 + U + \frac{U^2}{6} - X^2\right). \tag{4.31}$$

To determine X in terms of U, we combine these two equations and get the differential equation:

$$\frac{dX}{dU} = \frac{X}{U}\left(1 + \frac{3}{8X}\frac{d\log V}{d\Phi}\right). \tag{4.32}$$

If we assume $V(\Phi)$ behaves as an exponential in the IR-limit and use the ansatz $V(\Phi) = \exp(\rho\phi)$, we find:

$$\frac{dX}{dU} = \frac{X}{U}\left(1 + \frac{3\rho}{8X}\right).$$

This has a simple solution of the form:

$$X = kU - \frac{3\rho}{8},$$

where k is an integration constant.

4.3 Confinement Conditions

From here on, we will often consider the model in terms of the conformal coordinates (r, t, x). The equations of motion Eqs. [4.4-4.8] are rewritten below in terms of these coordinates:

$$A'' - A'^2 - A'W' - \frac{2}{3}W'^2 + \frac{4}{9}\phi'^2 + \frac{2}{3}B^2 Z e^{-2A-2W} = 0 \tag{4.33}$$

$$3A'W' - 2B^2 Z e^{-2A-2W} + W'' + 3W'^2 = 0 \tag{4.34}$$

$$\begin{aligned} &12A'W' + 12A'^2 + 2B^2 Z e^{-2A-2W} \\ &+ V e^{2A-2W} + 2W'^2 - \frac{4\phi'^2}{3} = 0. \end{aligned} \tag{4.35}$$

$$3A'\phi' - \frac{3}{4}B^2 Z' e^{-2A-2W} - \frac{3}{8}e^{2A-2W}V' + 3W'\phi' + \phi'' = 0. \tag{4.36}$$

To determine U_H, we consider some further restrictions to our model caused by quark confinement. As mentioned in Section 3.3, we need the distance L between a quark-antiquark pair, which is given by Eq. 3.23 to diverge.

If we consider the metric given by Eq. 4.3 in the ground state scenario, consider conformal coordinates work in the string frame, we obtain:

$$ds^2 = e^{2A_S}\left(e^{-2W}dr^2 - e^{2W}dt^2 + e^{2W}dx_3^2 + dR_2^2\right), \tag{4.37}$$

where $A_S \equiv A + \frac{2}{3}\phi$. By using Eq. 3.20, we find that if we consider a Wilson Loop in the direction parallel to x_3, the $f(r)$ and $g(r)$ are given by:

$$\begin{aligned} f^2(r) &= \exp(4A_S(r) + 4W(r)) \\ g^2(r) &= \exp(4A_S(r)) \end{aligned} \tag{4.38}$$

Therefore, L is given by:

$$L = 2\int_{r_B}^{r_F} dr\, e^{-2W(r)} \frac{1}{\sqrt{\exp(4A_S(r) + 4W(r) - 4A_S(r_F) - 4W(r_F)) - 1}} \tag{4.39}$$

Expanding the integrand around r_F gives:

$$\begin{aligned} &e^{-2W(r)} \frac{1}{\sqrt{\exp(4A_S(r) + 4W(r) - 4A_S(r_F) - 4W(r_F)) - 1}} = \\ &\exp(-2W(r_F)) \frac{1}{\sqrt{4(A_S'(r_F) + W'(r_F))(r - r_F) + 2(A_S''(r_F) + W_S''(r_F))(r - r_F)^2}} \end{aligned} \tag{4.40}$$

For L to diverge, the integrand needs to at least diverge as $\frac{1}{|r - r_F|}$, so we need $A_S(r) + W(r)$ to have a minimum at r_F.

We can do a similar analysis for Wilson Loops in a space transverse to the x_3-direction. For these Loops, we have:

$$\begin{aligned} f^2(r) &= \exp(4A_S(r) + 2W(r)) \\ g^2(r) &= \exp(4A_S(r)) \end{aligned} \tag{4.41}$$

$$L = 2\int_{r_B}^{r_F} dr\, e^{-W(r)} \frac{1}{\sqrt{\exp(4A_S(r) + 2W(r) - 4A_S(r_F) - 2W(r_F)) - 1}}. \tag{4.42}$$

After expanding the integrand around r_F, we find that for L to diverge, $2A_s(r) + W(r)$ must have a minimum at r_F.

In conclusion, quark confinement in the direction parallel to the magnetic field requires for $A_s(r) + W$ to have a minimum at a certain point r_F, while quark confinement in the direction transverse to the magnetic field requires for $2A_s(r) + W(r)$ to have a minimum.

4.4 Boundary Conditions

4.4.1 IR Limit

With the requirement that $A_S + W$ and $2A_S + W$ have a minimum, we get an extra restriction for the scalars. As we will show later in Section 4.4.2, $A'_S + W'$ and $2A'_s + W'$ are negative near the UV boundary. To have a minimum in $A_S + W$ and $2A_S + W$, we therefore require $A'_S + W'$ and $A'_s + 2W'$ to be positive in the IR-limit.

Before, we have shown that in the case that $B^2 H^2 Z(\phi)$ is negligible in the IR-limit, $X(\phi)$ and $U(\phi)$ are related by $X(\phi) = kU(\phi) - \frac{3\rho}{8}$, where k is an integration constant and $\rho = \frac{d \log V}{d\phi}$.

Substituting this expression for X in Equation 4.31, gives:

$$\frac{dU}{d\phi} = \frac{-4U}{3(kU - \frac{3}{8}\rho)} \left(1 + U + \frac{U^2}{6} - (kU - \frac{3}{8}\rho)^2\right) \tag{4.43}$$

Integration then shows that:

$$\phi - \phi_0 = \int_{U_0}^{U} \frac{3\left(kU - \frac{3}{8}\rho\right)}{-4U\left(1 + U + \frac{U^2}{6} - (kU - \frac{3}{8}\rho)^2\right)}\, dU = f(U) - f(U_0) \tag{4.44}$$

With

$$f(U) = \frac{3}{64 - 9\rho^2}\left(3\rho\left(\log(U^2) - \log(\gamma^2)/2\right) - 6\frac{16k + 3\rho}{\delta}\log\left(\left(\frac{1+\sigma}{1-\sigma}\right)^2\right)\right) \tag{4.45}$$

and

$$\sigma \equiv \frac{-12 - 24U + 24k^2U - 9k\rho}{\delta}$$

$$\gamma \equiv 192 - 32\left(6k^2 - 1\right)U^2 - 27\rho^2 + 48U(4 + 3k\rho)$$

$$\delta \equiv \sqrt{48 + 576k^2 + 216k\rho + \frac{27}{2}\rho^2} \tag{4.46}$$

From Equation 4.33, $X(\phi)$ can also be determined separately. If we divide by $A(r)^2$ and set Y and $B^2H^2Z(\phi)$ to zero, we find that:

$$\frac{\ddot{A}}{(\dot{A})^2} - 1 - U - \frac{2U^2}{3} + 4X^2 = 0.$$

Since X is assumed to be negative for all ϕ, we finally obtain:

$$X = -\frac{1}{2}\sqrt{1 + U + 2U^2/3 - \frac{\ddot{A}}{(\dot{A})^2}}. \tag{4.47}$$

For $A(r)$ in the IR-limit, we choose the following ansatz:

$$A(r) = -cr^\alpha, \tag{4.48}$$

where α and c are positive constants. This allows us to rewrite $\frac{\ddot{A}(r)}{\dot{A}(r)^2}$ as

$$\frac{\ddot{A}}{(\dot{A})^2} = \frac{\alpha - 1}{\alpha}\frac{1}{-cr^\alpha} \tag{4.49}$$

and we find that in as $r \to \infty$, $\frac{\ddot{A}}{(\dot{A})^2}$ converges to 0. By using Eq. 4.47 we find that X therefore converges to

$$X_h = \frac{-1}{2}\sqrt{1 + U_h + 2U_h^2/3} \tag{4.50}$$

as $r \to \infty$.

Considering Eq. 4.44 once more, we find that as $\phi \to \infty$ the right-hand side should diverge to $+\infty$. This only happens if $U \to \pm\infty$, $U \to 0$ (in which case $U = 0$ for all ϕ) or if U converges to a constant $c_{k,\rho}$ where $c_{k,\rho}$ either satisfies $\gamma = 0$ or $\sigma = \pm 1$.

In the case $U \to -\infty$, we find that $W(r)$ grows much faster than $A(r)$ decreases. As a result the entropy which behaves like $\exp(3A(r) + W(r))$ diverges. Therefore, $U \to -\infty$ is not an option.

For $U \to \infty$, we also get complications. As we mentioned before $A'_s + W'$ and $2A'_s + W'$ should be positive in the IR-limit is we want to have quark confinement. However, after rewriting $A'_s + W'$ as $A'_s + W' = A'(1 + 2X + U)$ and using that $X \to \frac{-1}{2}\sqrt{1 + U_h + 2U_h^2/3}$ in the IR-limit, we find $A'_s + W' \sim A'\left(1 - \sqrt{1 + U_h + 2U_h^2/3} + U_h\right)$ as $r \to \infty$. After sending $U_h \to \infty$, this approximates $(-\sqrt{2/3}U_h + U_h)A'$ which is negative. Therefore, $U \to \infty$ contradicts the requirement of quark confinement. This only leaves:

1. $U \to c_{k,\rho}$ as $(\phi \to \infty)$
2. $U \to 0$ as $(\phi \to \infty)$

We will now discuss both cases seperately.

Case $U \to c_{k,\rho}$

As mentioned before, $c_{k,\rho}$ must satisfy either $\gamma = 0$, $1 + \sigma = 0$ or $1 - \sigma = 0$. Furthermore, we can also use Eq. 4.50 to find the relation $kc_{k,\rho} - 3\rho/8 = -\frac{1}{2}\sqrt{1 + c_{k,\rho} + 2c_{k,\rho}^2/3}$. Solving these requirements leaves only one possible value for $c_{k,\rho}$, namely:

$$c_{k,\rho} = -1. \tag{4.51}$$

From the relation $kc_{k,\rho} - 3\rho/8 = -\frac{1}{2}\sqrt{1 + c_{k,\rho} + 2c_{k,\rho}^2/3}$, we then find that k is given by $k = \frac{1}{\sqrt{6}} - \frac{3\rho}{8}$.

Furthermore, the requirement that $B^2H^2Z(\phi) \to 0$ in the IR-limit gives a restriction to the value of ρ. To show this, we start from the definition of $B^2H^2Z(\phi)$ to rewrite:

$$\lim_{\phi\to\infty} B^2H^2Z = \lim_{\phi\to\infty} \frac{B^2 Z_0 \exp(\sigma\phi - 2A - 2W)}{\dot{A}^2}$$
$$= \lim_{\phi\to\infty} \frac{B^2 Z_0 \exp((3X\sigma - 2 - 2U)A}{\dot{A}^2} = \lim_{\phi\to\infty} \frac{B^2 Z_0 \exp(-\frac{3}{\sqrt{6}}\sigma A)}{\dot{A}^2}$$

This only goes to zero if $\sigma \leq 0$. Through the boundary $X_h = \frac{-3}{8}\rho + \frac{U_h}{8}(\sigma - 2\rho)$ we find that this implies that $\rho \geq 4\sqrt{2/3}$.

We can refine this condition further by showing that $\rho > 4\sqrt{2/3}$ is not an option. To do this, we substitute $k = \frac{1}{\sqrt{6}} - \frac{3\rho}{8}$ in the solution for $\phi(U)$. This gives:

$$\phi(U) = \frac{9\rho}{64 - 9\rho^2}\log(U^2) + \frac{1}{2(\rho - 4\sqrt{2/3})}\log((1+U)^2)$$
$$+\frac{9}{2}\frac{(9 - 4\sqrt{2/3} + 4\sqrt{2/9})(9 - 4\sqrt{2/3} - 4\sqrt{2/9})}{(9\rho^2 - 64)(\rho - 4\sqrt{2/3})}\log((64 - 9\rho^2 + 8\sqrt{6}U\rho - 9U\rho^2)^2).$$

For $\rho > 4\sqrt{2/3}$, we find that the prefactor of $\log((1+U)^2)$ is positive, therefore $\phi(-1) \to -\infty$ while we want $\phi(-1) \to \infty$. This only leaves $\rho = 4\sqrt{2/3}$ as a solution for ρ, so the potential is now given by:

$$V(\phi) = V_0 \exp(4\sqrt{2/3}\phi) \tag{4.52}$$

in the IR-limit.

With ρ determined as $\rho = 4\sqrt{2/3}$, σ and k are fixed as $\sigma = 0$ and $k = \frac{1}{\sqrt{6}} - \sqrt{3/2}$. Substituting these values directly into the solution $\phi(U)$, returns a singularity. However, if we substitute these values first in Eq. 4.31 and solve it afterwards, we find: $\phi(U) - \phi_0 = f(U) - f(U_0)$ with

$$f(U) = -\frac{1}{4\sqrt{2/3}}\left(\frac{2}{1+U} + 3\log(U^2) - 3\log((1+U)^2)\right)$$

For $\phi \gg 1$, we can now approximate $U(\phi)$ with $U(\phi) \approx -1 + \frac{1}{\sqrt{8/3}}\frac{1}{\phi}$.
To determine how $U(\phi)$ converges to -1, we expand $W(r)$ as $W(r) = -A(r) + W_1 \log|A(r)|$. $U(r)$ is now given by $U = -1 + \frac{W_1}{A(r)}$, where W_1 is a constant yet to be determined. This can be done by dividing the equation of motion Eq. 4.34 by $A'(r)^2$ and substitute the expressions for $W(r)$ and $A(r)$. This gives:

$$\frac{W''(r)}{A'(r)^2} + 3U(1+U) + B^2H^2Z = \frac{-A''(r) + W_1(\frac{A''(r)}{A'(r)} - 1)}{A'(r)^2} - 3(-1 + \frac{W_1}{A(r)})\frac{W_1}{A(r)} = 0$$

and is solved by requiring $W_1 = \frac{-1}{3}\frac{\alpha-1}{\alpha}$. Therefore, $U \sim -1 - \frac{1}{3}\frac{\alpha-1}{\alpha}\frac{1}{A(r)}$.

With the behaviour of $U(r)$ now known, we can substitute this expression of U in Eq.4.50. This then returns:

$$X(r) \to \frac{-1}{\sqrt{6}} + \frac{1}{3}\sqrt{\frac{2}{3}}\frac{\alpha-1}{\alpha}\frac{1}{A(r)}.$$

From the definitions of the scalars, $\phi'(r)$ and $W'(r)$ can be written in terms of $A(r)$. Integration then gives:

$$\phi(r) = \phi_h + \frac{-3}{\sqrt{6}}A(r) + \sqrt{\frac{2}{3}}\frac{\alpha-1}{\alpha}\log|A(r)|$$
$$W(r) = W_h - A(r) + \frac{1}{3}\log|A(r)|.$$

Since we found for $Z(\phi) = \exp(\sigma\phi)$ the value $\sigma = 0$, we consider Equation 4.33 once more to find a ϕ-dependent expression for Z. For now, we assume $Z(\phi)$ to be a given by a power law $Z(\phi) = Z_0\phi^\epsilon$. Substituting the expressions for $A(r)$, $\phi(r)$ and $W(r)$ into Eq. 4.33 gives:

$$\begin{aligned}A''(r) - 1 - A'(r)W'(r) - \frac{2}{3}W'(r)^2 + \frac{4}{9}\phi'(r)^2 + \frac{2}{3}B^2 Z(\phi)\exp(-2A(r) - 2W(r))\\ = \frac{2(\alpha-1)^2}{9r^2} + \frac{2}{3}B^2 Z_0\phi^\epsilon|A(r)|^{\frac{2(\alpha-1)}{3\alpha}} = 0\end{aligned} \tag{4.53}$$

Because $A(r)$ and $\phi(r)$ are of order r^α, we find that for the second term to be of order r^{-2}, ϵ should be given by $\epsilon = -\frac{2}{3}\frac{\alpha+2}{\alpha}$. Therefore, $Z(\phi)$ is given by:

$$Z(\phi) = Z_0\phi^{-\frac{2}{3}\frac{\alpha+2}{\alpha}}. \tag{4.54}$$

We now have an expression for all the fields and potentials in the IR-limit in the case that U converges to a value $c_{k,\rho} \neq 0$. However, we should note that the potential $V(\phi)$ behaves differently in the IR-limit than in the case $B = 0$. To show this, we note that in the case $B = 0$, the model reduces to the model described in Section 3.2. As shown in [20], $V(\phi)$ behaves in this model as $V(\phi) \to \exp(4\phi/3)$ as $r \to \infty$. Since we do not want the potential V to be dependent on B, we consider the case $U \to 0$ as $r \to \infty$ instead.

Case $U \to 0$

For $A = -cr^{-\alpha}$ and $U = 0$, we find that

$$X = -\frac{1}{2}\sqrt{1 - \frac{\ddot{A}}{(\dot{A})^2}} \approx -\frac{1}{2} + \frac{\ddot{A}}{4(\dot{A})^2} = \frac{-1}{2} + \frac{1}{4}\frac{\alpha - 1}{\alpha}\frac{1}{A(r)}$$

By making use of the definitions of the scalars, we find $\phi'(r) = 3XA'(r) = \frac{-3A'(r)}{2} + \frac{3}{4}\frac{\alpha-1}{\alpha}\frac{A'(r)}{A(r)}$ and $W'(r) = 0$. Therefore:

$$\phi(r) = \frac{-3}{2}A(r) + \frac{3}{4}\frac{\alpha - 1}{\alpha}\log(A(r))$$

$$W(r) = W_h,$$

as $r \to \infty$, with W_h a constant. However, if both $U = 0$ and $B^2H^2Z(\phi) = 0$ in the IR limit, Eq. 4.17 shows that this is the case for the whole domain of Φ. However, this removes all dependency on the magnetic field in our model, which is not what we want.

As a solution to this problem, we consider instead of a negligible value of $B^2H^2Z(\phi)$ a function which converges to 0 in the IR-limit, but is relevant in the equations of motion.

From Eq. 4.34 we already obtain a relation between U and $B^2H^2Z(\phi)$. Since $U \ll 1$ in the IR-limit, we find that the leading order term $3A'(r)W'(r)$ can only be cancelled by the term $2B^2e^{-2A-2W}$. This implies that U is of the same order as $B^2H^2Z(\phi)$ in the IR-limit. In particular, we find the relation $B^2H^2Z(\phi) = \frac{3}{2}U(\phi)$.

To find an expression for $X(\phi)$, $U(\phi)$ and $B^2H^2Z(\phi)$ in the IR-limit, we substitute the ansatz $X(\phi) = -\frac{1}{2} + \frac{X_0}{\phi} + \frac{X_1}{\phi^2}$, $U(\phi) = \frac{U_0}{\phi} + \frac{U_1}{\phi^2}$ and $B^2H^2Z(\phi) = \frac{\lambda_0}{\phi} + \frac{\lambda_1}{\phi^2}$ in the scalar equations of motion. For the potential $V(\phi)$ we allow a correction in the form of a power law, such that $V(\phi)$ is now given by $V(\phi) = V_0\exp(4\phi/3)\phi^{V_1}$. Lastly, to aqcuire an expression for $Z(\phi)$ we first consider the definition of $B^2H^2Z(\phi)$. Because

$$B^2H^2Z(\phi) = B^2Z_0\frac{\exp(\sigma\phi - 2A - 2W)}{(A')^2} \sim B^2Z_0\frac{\exp((3X\sigma - 2)A}{(A')^2}$$

and X converges to $\frac{-1}{2}$. We find that $B^2H^2Z(\phi)$ behaves like

$$B^2 Z_0 \frac{\exp(-(-3\sigma/2-2)cr^\alpha}{(A')^2}$$

in the IR-limit. Since we want to be able to write B^2H^2Z in terms of order ϕ^{-1} and order ϕ^{-2}, it should not converge like e^{-cr} with $c \neq 0$. The only value of σ for which this is the case is $\sigma = -4/3$. Also here, we allow a correction in the form of a power law for Z, which results in the following ansatz:

$$Z(\phi) = Z_0 \exp(-4\phi/3)\phi^{Z_1}.$$

Substituting all these definitions in Eqs. 4.15-4.18 and setting the left-hand side equal to the right-hand side of the equations gives the following solution:

$$\begin{aligned} X(\phi) &= -\frac{1}{2} - \frac{3}{16\phi} + \left(-\frac{X_0}{2} - \frac{\lambda_1}{3}\right)\frac{1}{\phi^2} \\ U(\phi) &= \frac{2\lambda_1}{3\phi^2} \\ B^2H(\phi)^2Z(\phi) &= \frac{\lambda_1}{\phi^2} \\ V(\phi) &= V_0 \exp(4\phi/3)\phi^{-8X_0/3} \\ Z(\phi) &= Z_0 \exp 4\phi\phi^{8X_0/3}, \end{aligned} \tag{4.55}$$

where X_0 is given by $X_0 = -\frac{3}{8}\frac{\alpha-1}{\alpha}$. Indeed, we find that $B^2H^2Z(\phi) \sim \frac{3}{2}U(\phi)$ in the IR-limit.

Substituting these solutions in Eq. 4.33 and using $A(r) = -cr^\alpha$ then gives:

$$\begin{aligned} \phi(r) &= \phi_h + \frac{3}{2}cr^\alpha + \frac{3}{4}\log(r^{\alpha-1}) + 7\mathcal{O}(r^-\alpha) \\ W(r) &= W_h + \frac{8\lambda_1}{27}\frac{1}{cr^\alpha} + \mathcal{O}r^{-2\alpha} \end{aligned} \tag{4.56}$$

With the results for $A(r), \phi(r)$ and $W(r)$ now determined, we can check if there are extra restrictions cause by confinement. Direct calculations shows that:

$$A'_s + W' = -c\alpha r^{\alpha-1} + c\alpha r^{\alpha-1} + \frac{(\alpha-1)}{2r} - \frac{8\alpha\lambda_1}{27}\frac{1}{cr^{a+1}} = \frac{(\alpha-1)}{2r} - \frac{8\alpha\lambda_1}{27}\frac{1}{cr^{a+1}}$$

$$2A_s'+W' = -2c\alpha r^{\alpha-1}+2c\alpha r^{\alpha-1}+\frac{(\alpha-1)}{r}-\frac{8\alpha\lambda_1}{27}\frac{1}{cr^{a+1}} = \frac{(\alpha-1)}{2r}-\frac{8\alpha\lambda_1}{27}\frac{1}{cr^{a+1}}$$

So for confinement, we need $\alpha \geq 1$. This is the same restriction as was obtained in the case without an external magnetic field as shown in [20].

For $B = 1$ and $\lambda_1 = -0.1815^2$, the results to the scalar equations with these boundary conditions in the IR-limit are shown in Figure 4.1. We find that $X(\phi)$ indeed approaches $-\frac{1}{2}$ from below and that U and $B^2H^2Z(\phi)$ quickly converge to zero.

4.4.2 UV Limit

In the UV limit, the leading term of $A(r)$ is given by $A(r) = -\log(r)$ to ensure the metric resembles AdS_5 in this region. Using this as a starting point, we expand $Z(\phi)$ as $Z(\phi) = Z_0 + Z_1\phi + \mathcal{O}(\phi^2)$ and consider Eq. 4.34. This gives:

$$W''(r)-3\frac{W'(r)}{r}+3W'(r)^2-2B^2r^2(Z_0+Z1\phi(r))\exp(-2W(r)) = 0 \quad (4.57)$$

The leading order terms of this equation are given by:

$$W''(r) - 3\frac{W'(r)}{r} - 2B^2r^2Z_0\exp(-2W(r)) + \mathcal{O}(r^4) = 0. \quad (4.58)$$

After solving this differential equation, we find that $W(r)$ approximates:

$$W(r) = W_c r^4 \log(r) + \mathcal{O}(r^4)$$

with

$$W_c = \frac{B^2Z_0}{2}.$$

With the knowledge that $W(r) = \mathcal{O}(r^4)$ in the UV-limit, we find that the leading terms of Eq. 4.36 are now given by:

$$\phi''(r) + 3\phi'(r)A(r) + \frac{3}{8}V'(\phi(r)) = 0. \quad (4.59)$$

After expanding $V(\phi)$ as $V(\phi) = V_0 - \frac{m^2}{2}\phi^2$ in this region, we find that this equation is solved by:

$$\phi(r) = c_1r^{2(1+\sqrt{1-\frac{3}{32}m^2})} + c_2r^{2(1-\sqrt{1-\frac{3}{32}m^2})}. \quad (4.60)$$

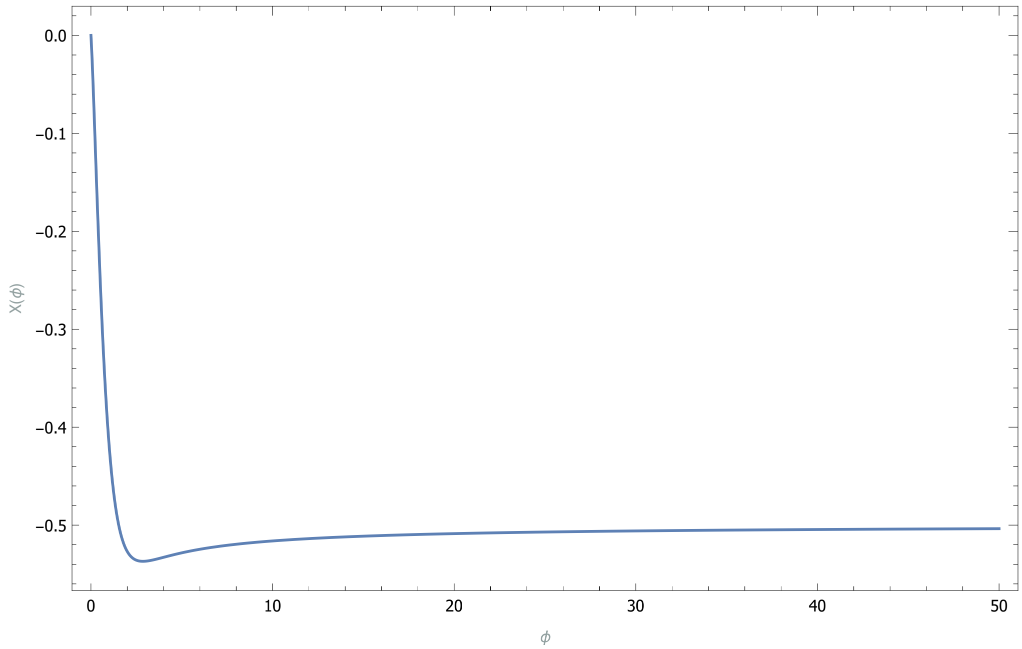

(a) $X(\phi)$ as a function of ϕ

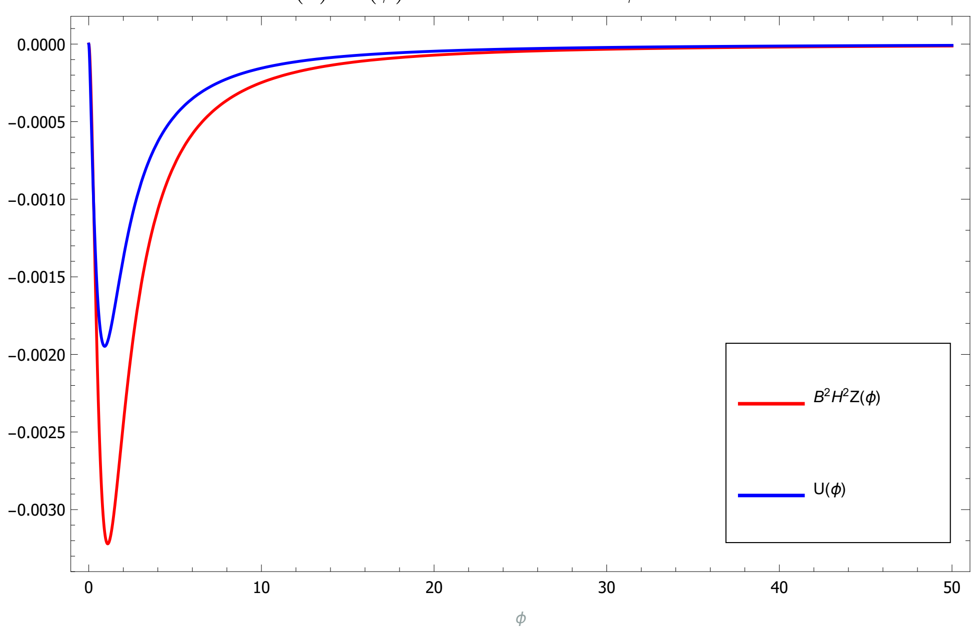

(b) $U(\phi)$ (blue) and $B^2H(\phi)^2Z(\phi)$ (red) as a function of ϕ

Figure 4.1: The scalars $X(\phi)$, $U(\phi)$ and the function $B^2H(\phi)^2Z(\phi)$ as a function of ϕ in the case $B = 1$ and $\lambda_1 = 0.1815$.

For the scaling dimension of ϕ, this gives the following relation:

$$\frac{3}{8}m^2 = \Delta(4-\Delta), \tag{4.61}$$

where m is the mass of the dilaton.

For now we choose $\Delta = 3$, which gives $m^2 = 8$ and we find that $V(\phi)$ is given by:

$$V(\phi) = V_0 - 4\phi(r)^2.$$

Substituting these expressions in Eq. 4.35 shows that $V_0 = -12$ in order to let the terms scaling with $\frac{1}{r^2}$ cancel. As the scaling dimension is given by $\Delta = 3$, $\phi(r)$ satisfies:

$$\phi(r) = \phi_0 r + \phi_1 r^3, \tag{4.62}$$

in the UV-limit, where ϕ_0 and ϕ_1 are constants.

To find a more precise description of $A(r)$ near the boundary, we also include a term scaling with r^2. In other words, we assume $A(r) = -\log(r) + A_2 r^2$. Eqs. 4.33 and 4.35 now return:

$$\left(6A_2 + \frac{4}{9}\phi_0^2\right) + \mathcal{O}(r^2) = 0 \tag{4.63}$$

$$\left(-72A_2 - \frac{16}{3}\phi_0^2\right) + \mathcal{O}(r^2) = 0 \tag{4.64}$$

Therefore, we find that $A_2 = -\frac{2}{27}\phi_0^2$.

Lastly, we include terms proportional to r^4 to the expression of $A(r)$ to also cancel the leading order terms involving $W(r)$. For this, we consider the ansatz $A(r) = -\log(r) - \frac{2}{27}\phi_0^2 r^2 + A_3 r^4 + A_4 \log(r) r^4$.

Substituting the expressions for $A(r), \phi(r)$ and $W(r)$ in Eq. 4.33 gives:

$$\left(20A_4 + 2B^2 Z_0\right)\log(r)r^2 + \left(20A_3 + 9A_4 - \frac{16}{729}\phi_0^4 + \frac{8}{3}\phi_0\phi_1 + \frac{7}{6}B^2 Z_0\right)r^2 = 0, \tag{4.65}$$

which results in $A_4 = \frac{-B^2 Z_0}{10}$ and $A_3 = \frac{4}{3645}\phi_0^4 - \frac{2}{15}\phi_0\phi_1 - \frac{B^2 Z_0}{75}$.

In summary, we obtained to following expressions:

$$\begin{aligned} A(r) &= -\log(r) - \frac{2}{27}\phi_0^2 r^2 + \left(\frac{4}{3645}\phi_0^4 - \frac{2}{15}\phi_0\phi_1 - \frac{B^2 Z_0}{75}\right) r^4 - \frac{B^2 Z_0}{10}\log(r) r^4 \\ W(r) &= \frac{B^2 Z_0}{2}\log(r) r^4 \\ \phi(r) &= \phi_0 r + \phi_1 r^3 \end{aligned} \tag{4.66}$$

With the UV and IR behaviour of $V(\phi)$ determined, we can construct an expression for $V(\phi)$ which satisfies both these boundary conditions. In our calculations, we consider the case $\alpha = 2$. Here, $V(\phi)$ is proportional to $\exp(4\phi/3)\sqrt{\phi}$ in the IR limit. To determine $V(\phi)$ fully, we start from the ansatz:

$$V(\phi) = \alpha \exp(\gamma\phi) + \beta \exp(4\phi/3)\sqrt{1+\phi},$$

expand it around $\phi = 0$ and demand that this expansion satisfies $V(\phi) = -12 - 4\phi^2$ for low ϕ. This fixes the values of α, β and γ as:

$$\alpha = -\frac{2904}{163 + \sqrt{17857}}$$

$$\beta = \frac{-12\sqrt{17857} + 948}{163 + \sqrt{17857}}$$

and

$$\gamma = -\frac{\sqrt{17857} - 79}{132} \tag{4.67}$$

Lastly, as we had no clear restriction for $Z(\phi)$ in the UV-limit, we use the IR dynamics of $Z(\phi)$ and let $Z(\phi)$ be given by:

$$Z(\phi) = Z_0\sqrt{1+\phi}\,e^{-4\phi/3}. \tag{4.68}$$

4.5 Solving to the Equations of Motion

From the solutions of the scalar fields in terms of ϕ we can calculate the fields $A(r)$, $\phi(r)$ and $W(r)$. To do this, we divide Eq. 4.33 by $A'(r)^2$ and replace the fields with the scalars where possible. This leaves:

$$\frac{A''(r)}{A'(r)^2} - 1 - U - \frac{2U^2}{3} + 4X^2 + \frac{2}{3}B^2 H^2 Z(\phi) = 0. \tag{4.69}$$

The term $\frac{A''(r)}{A'(r)^2}$ can be rewritten as $\frac{A''(r)}{A'(r)^2} = \frac{d\log(\frac{dA}{dr}(\phi)}{d\phi}3X(\phi)$. Therefore, we find that:

$$\frac{d\log(\frac{dA}{dr}(\phi)}{d\phi} = \frac{1 + U + \frac{2U^2}{3} - 4X^2 - \frac{2}{3}B^2H^2Z(\phi)}{3X}. \tag{4.70}$$

By solving this equation, we obtain $\frac{dA}{dr}$ as a function of ϕ. Then, by using the definition of X, we can then write $\frac{d\phi}{dr}$ as a function of ϕ. After solving this, we get an expression for $\phi(r)$. With $\phi(r)$ known, $\frac{dA}{dr}$ can be determined in terms of r by substituting the expression of $\phi(r)$ and we obtain $A(r)$ by a simple integration. Lastly, we can obtain $W(r)$ through the definition $U = \frac{W'(r)}{A'(r)}$ and the newly found expressions of $A(r)$ and $\phi(r)$.

One thing we should however make sure is that in the IR limit, the scalar value of $B^2H^2Z(\phi)$ corresponds with $B^2Z(\phi(r))\frac{\exp(-2A(r)-2W(r))}{A'(r)^2}$. For this, we use the fact that λ_1 is still a free parameter and vary this parameter until both expressions of $B^2H^2Z(\phi)$ match.

For $B = 1$, $B = 2$, $B = 3$ and $B = 4$ the results are shown Figs. **??**-**??**. We find that the absolute value of $A(r)$ and $\phi(r)$ both decrease as B. Furthermore, $W(r)$ increases for increasing B. For $A(r)$ we also seperately plotted the UV behaviour together with the function $-\log(r)$. As can be seen, the results of $A(r)$ match this function perfectly in the UV-limit.

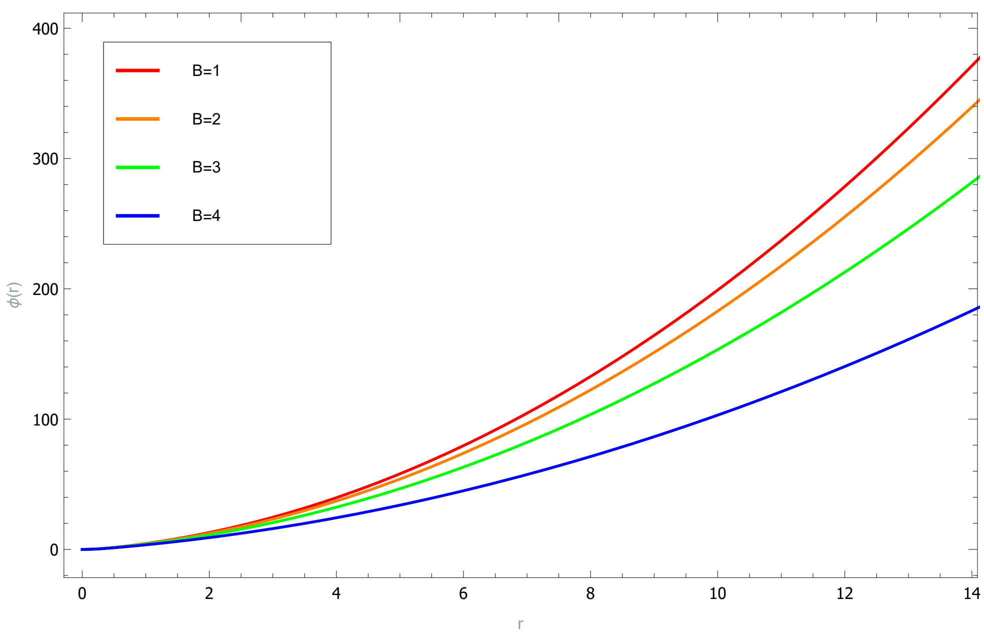

Figure 4.2: Plot of $\phi(r)$ for various values of B.

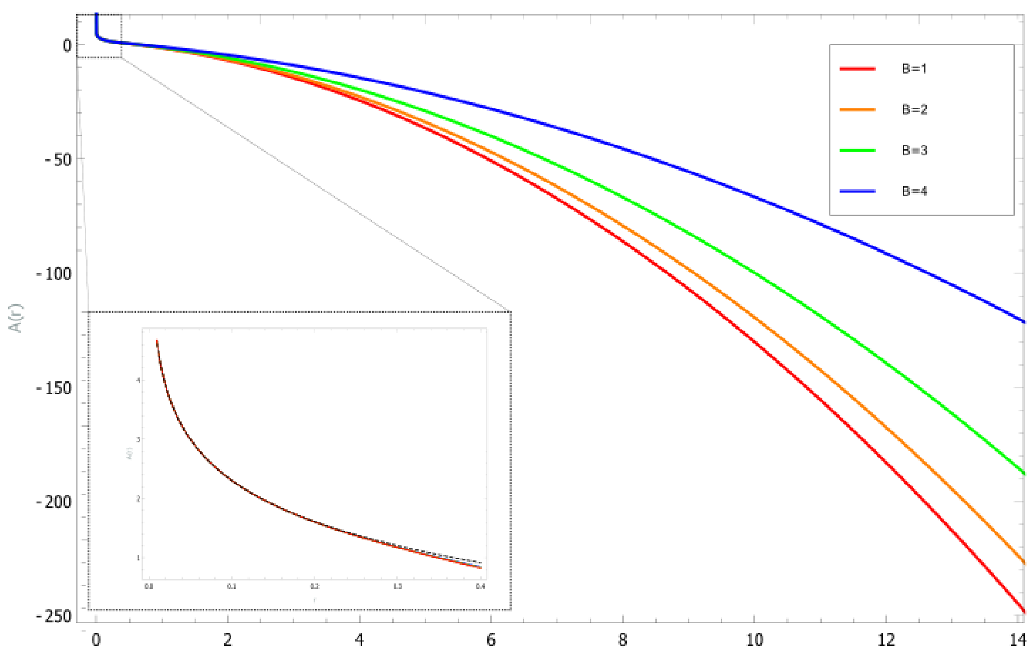

Figure 4.3: Plot of $A(r)$ for various values of B. In the inset, $A(r)$ is plotted for various values of B, together with the function $-\log(r)$. As can be seen here, there is a good overlap between this function and $A(r)$ in this limit for all the values of B we consider.

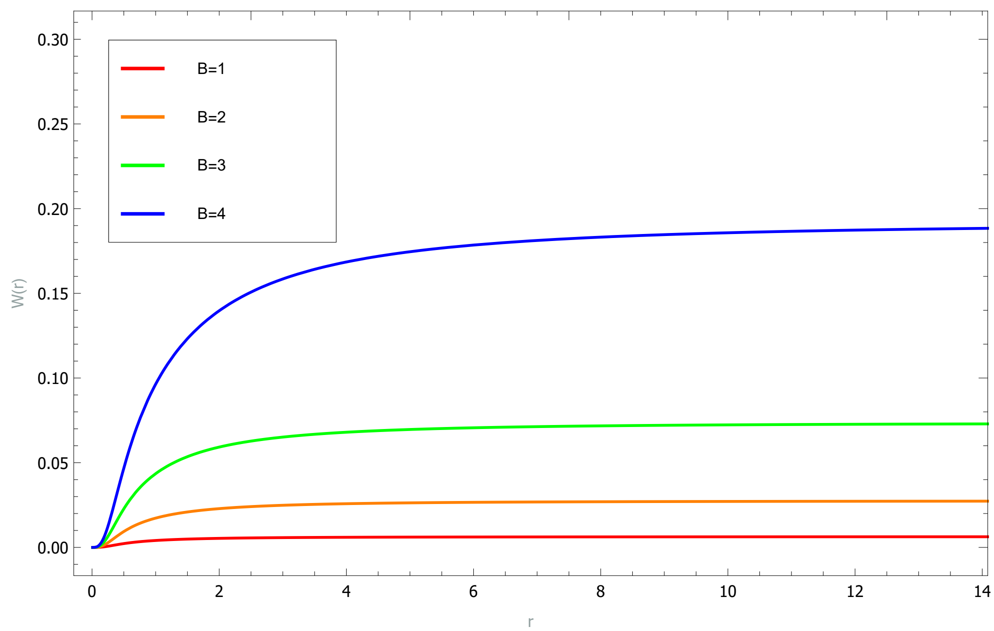

Figure 4.4: Plot of $W(r)$ for various values of B.

Chapter 5

Mass Spectrum

As discussed in Section 3.4, to find the mass spectrum, we need to solve the fluctuation equation $\xi''(r) + 2B'(r)\xi'(r) + m^2\xi(r) = 0$. Just like there, we use $B(r) = \frac{3}{2}A(r) + \log|X(\phi(r))|$ to determine the $J^{PC} = 0^{++}$ glueballs and $B(r) = \frac{3}{2}A(r)$ to determine the $J^{PC} = 2^{++}$ glueballs. Furthermore, we assume that $\xi(r)$ behaves like $\xi(r) = r^4$ in the UV-limit. Using the procedure mentioned in Section 3.4, we obtained the glueball spectrum for both these cases for various values of B. The results are shown in figure 5.1 and 5.2.

In contrast to what we know of Landau quantization, we find that the masses of the glueballs decrease with increasing values of B. We should take note however of the fact that Landau quantization is a theory for a system with weak coupling, so the fact that the masses decrease if increasing values of B can also be a result of the strong interactions. Furthermore, unlike the charged particles considered in Landau quantization, the glueballs are color charge neutral.

To find out whether this result was a specific to $\Delta = 3$, we performed the same calculations for $\Delta = 5/2$. Here, the boundary conditions in the UV-limit were given by:

$$\begin{aligned} A(r) &= -\log(r) - \frac{\phi_0^2}{12}r^3 - \frac{B^2 Z_0}{10}r^4\log(r) - \frac{1}{150}\left(25\phi_0\phi_1 + 2B^2 Z_0\right) \\ \phi(r) &= \phi_0 r^3/2 + \phi_1 r^5/2 \\ W(r) &= \frac{B^2 Z_0}{2}r^4\log(r). \end{aligned} \tag{5.1}$$

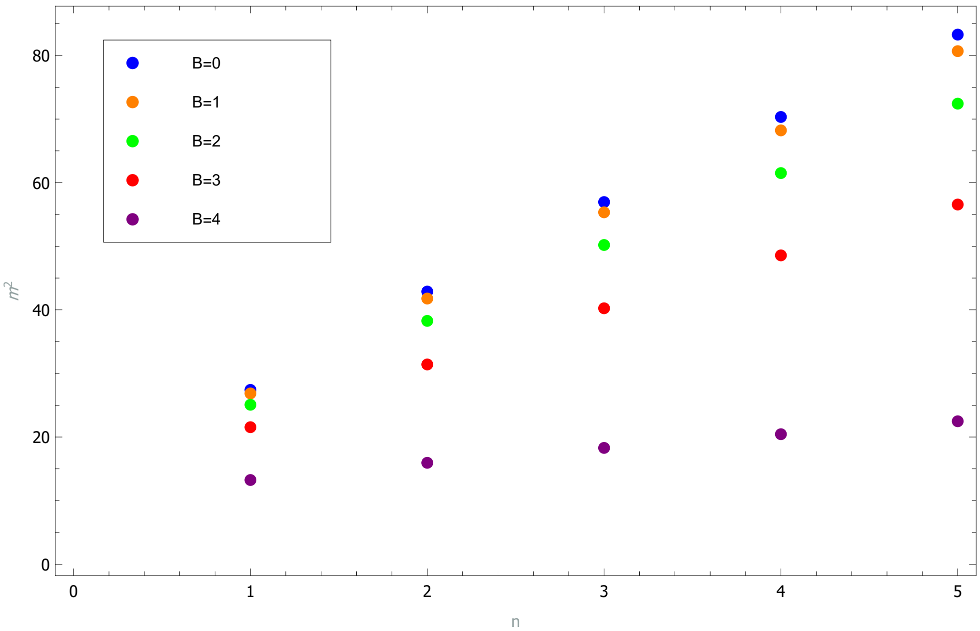

Figure 5.1: Spectrum for 2^{++} glueballs. The parameters used are $\Delta = 3$, $\phi_0 = 1.2$, $Z_0 = -1$ and $\phi_1 = 1$.

For the potential V we used:

$$V(\phi) = \alpha \exp(\gamma\phi) + \beta\sqrt{1+\phi}\exp(-4\phi/3), \tag{5.2}$$

with:

$$\begin{aligned}\alpha &= -\frac{169+\sqrt{19849}}{3}\\ \beta &= \frac{133-\sqrt{19849}}{3}\\ \gamma &= \frac{73-\sqrt{19849}}{132}\end{aligned} \tag{5.3}$$

However, we found a similar trend for this value of Δ; the spectra still decreases for increasing values of B.

To find out if we can understand this mathematically, we study the behaviour of the Schrödinger potential corresponding to the fluctuations given by Eq. 3.32. The Schrödinger equation is slightly rewritten below:

$$\psi''(r) = (V_s(r) - m^2)\psi(r). \tag{5.4}$$

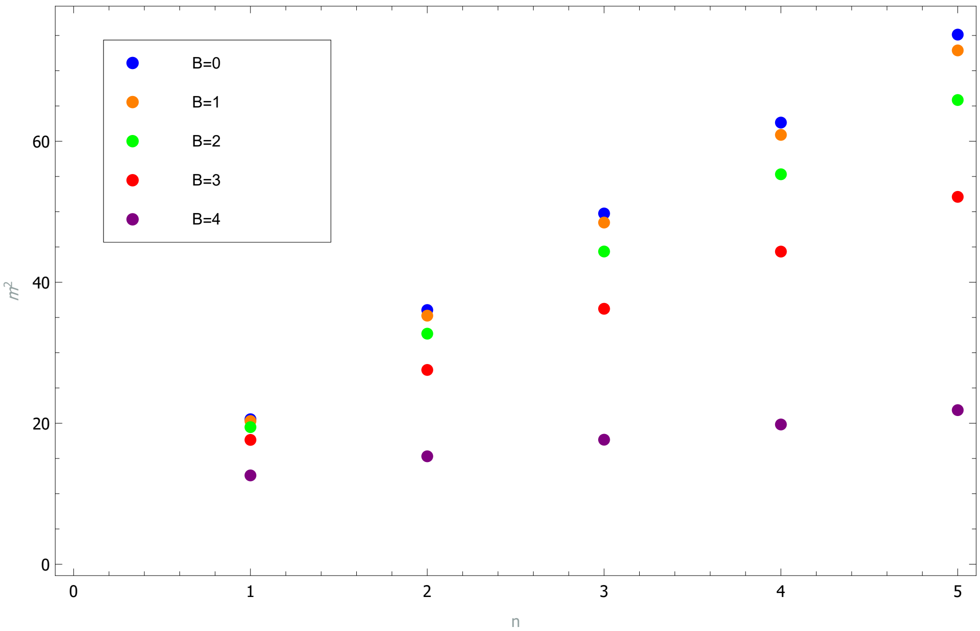

Figure 5.2: Spectrum for 0^{++} glueballs. Here, we used the parameters $\Delta = 3$, $\phi_0 = 1.2$, $Z_0 = -1$ and $\phi_1 = 1$

From this, we see that $\psi(r)$ oscillates when $V_s(r) < m^2$. Therefore, if the function $V_s(r)$ becomes lower, then the values of m^2 needed to ensure oscillating behaviour is also lower. As a result, the value of m^2 which is needed to let another node appear in the wave function, also decreases. In Fig. 5.3, the Schrödinger potential is shown for different values of B. As can be seen, the potential decreases for increasing values of B, which would explain the lowering of the spectra.

We can also confirm the decrease in the Schrödinger potential from the equations of motion. From Eq. 3.32 we can determine the Schrödinger potential in terms of $B(r)$. We find that for both the 0^{++} glueballs and the 2^{++} glueballs that the Schrödinger potential becomes quickly dominated by the term $B'(r)^2 = \frac{9}{4}A'(r)^2$ for large enough values of r. In our results this happened when $r \sim 2$. From Eq. 4.35, we find that :

$$12A'W' + 12A'^2 + 2B^2 Ze^{-2A-2W} + Ve^{2A-2W} + 2W'^2 - \frac{4\phi'^2}{3} = 0.$$

Using the fact that $\phi(r) \sim \frac{3}{2}A(r)$ for large enough values of r, we can rewrite

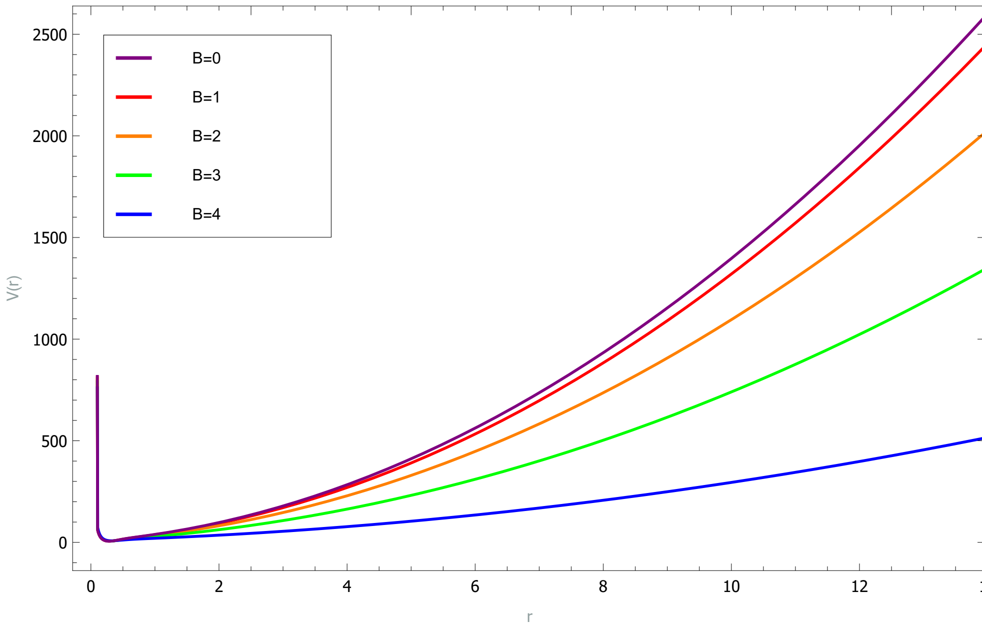

Figure 5.3: $V(r)$ for various values of B for $\phi_0 = 1.2$, $\phi_1 = 1$ and $\Delta = 3$

this as:

$$9A'^2 = -12A'W' - 2B^2 Z e^{-2A-2W} - V e^{2A-2W} - 2W'^2$$

On the right-hand side, the term $-Ve^{2A-2W}$ dominates and goes like r^2. As $V(\phi) \sim V_0\sqrt{\phi}\exp(4\phi/3)$ (with $V_0 < 0$) for large enough values of ϕ, the term $-Ve^{2A-2W}$ behaves as:

$$-Ve^{2A-2W} \sim -V_0\sqrt{\phi}\exp(4\phi/3)e^{2A-2W} \sim -V_0\exp(2W),$$

since $\phi(r) \sim \frac{3}{2}A(r)$. Because W increases with increasing values of B, $-V_0\exp(2W)$ decreases and thus $|A'(r)|$ and $V_s(r)$ both decrease for increasing values of B. This in turn causes the spectra to shift to lower values.

Physically, the reason for a decrease in mass is still unclear. We suspect however, that this has to do with the sea effect. This describes how the presence of the magnetic field strength in the determininant of the QFT gives a weighting to the different gauge formations [24]. The preference of certain configurations caused by this mechanism, could result in a decrease in the energy levels.

Chapter 6

Conclusion

In this project, we studied the effect of an external magnetic field on the glueball spectra. For this, we used improved holographic QCD to construct a toy model for pure Yang-Mills theory based on an Einstein-Maxwell-Dilaton action where the dilaton couples to a electromagnetic field tensor through a exponential coupling term. During the construction of the model, we ensured that quark-confinement is maintained, found a description for the ground state of the model and calculated the UV-boundary conditions for which the metric behaves like AdS_5 near the boundary.

From these restriction and boundary conditions, we obtained the relevant fields necessary to calculate the glueball spectra for various values of B. Surprisingly, we find that for increasing values of B, the masses decrease. This is in contrast with Landau levels, where the masses increase for increasing values of B.

For future research, it would be interesting to see if this trend of decreasing masses hold for different potentials $V(\phi)$ and different couplings $Z(\phi)$. It would also be interesting to study the physics behind the decreasing masses and find out how strong coupling plays a role in the decrease of masses.

Bibliography

[1] Brian Robert Martin. *Nuclear and particle physics*. Wiley Online Library, 2006.

[2] Harald Fritzsch. "History of QCD". In: *What we would like LHC to give us: Proceedings of the International School of Subnuclear Physics*. World Scientific, 2014, pp. 23–27.

[3] Vladimir A Miransky and Igor A Shovkovy. "Quantum field theory in a magnetic field: From quantum chromodynamics to graphene and Dirac semimetals". In: *Physics Reports* 576 (2015), pp. 1–209.

[4] F. Bruckmann et al. "Landau levels in QCD". In: *Phys. Rev. D* 96.7 (2017), p. 074506. DOI: 10.1103/PhysRevD.96.074506. arXiv: 1705.10210 [hep-lat].

[5] Falk Bruckmann et al. "Landau levels in QCD in an external magnetic field". In: *EPJ Web Conf.* 175 (2018). Ed. by M. Della Morte et al., p. 07014. DOI: 10.1051/epjconf/201817507014. arXiv: 1711.08720 [hep-lat].

[6] G. S. Bali et al. "The QCD phase diagram for external magnetic fields". In: *Journal of High Energy Physics* 2012.2 (Feb. 2012). ISSN: 1029-8479. DOI: 10.1007/jhep02(2012)044. URL: http://dx.doi.org/10.1007/JHEP02(2012)044.

[7] Michel Le Bellac. *Quantum physics*. Cambridge University Press, 2011.

[8] Michael E Peskin and Daniel V Schroeder. "An introduction to quantum field theory". In: (1995).

[9] Mark Thomson. *Modern particle physics*. Cambridge University Press, 2013.

[10] Umut Gursoy. "Improved holographic QCD and the quark-gluon plasma". In: *arXiv preprint arXiv:1612.00899* (2016).

[11] Rajan Gupta. “Introduction to lattice QCD”. In: *arXiv preprint hep-lat/9807028* (1997).

[12] Harvey B Meyer. “Glueball regge trajectories”. In: *arXiv preprint hep-lat/0508002* (2005).

[13] Martin Ammon and Johanna Erdmenger. *Gauge/gravity duality: Foundations and applications*. Cambridge University Press, 2015.

[14] Ofer Aharony et al. “Large N field theories, string theory and gravity”. In: *Physics Reports* 323.3-4 (2000), pp. 183–386.

[15] Edward Witten. “Anti-de Sitter space, thermal phase transition, and confinement in gauge theories”. In: *arXiv preprint hep-th/9803131* (1998).

[16] Joshua Erlich et al. “QCD and a holographic model of hadrons”. In: *Physical Review Letters* 95.26 (2005), p. 261602.

[17] Leandro Da Rold and Alex Pomarol. “Chiral symmetry breaking from five-dimensional spaces”. In: *Nuclear Physics B* 721.1-3 (2005), pp. 79–97.

[18] Andreas Karch et al. “Linear confinement and AdS/QCD”. In: *Physical Review D* 74.1 (2006), p. 015005.

[19] Marco Panero. “Thermodynamics of the QCD plasma and the large-N limit”. In: *Physical review letters* 103.23 (2009), p. 232001.

[20] U Gürsoy, E Kiritsis, and F Nitti. “Exploring improved holographic theories for QCD: Part II”. In: *Journal of High Energy Physics* 2008.02 (2008), p. 019.

[21] Juan Maldacena. “Wilson loops in large N field theories”. In: *Physical Review Letters* 80.22 (1998), p. 4859.

[22] David Tong. “Lectures on string theory”. In: *arXiv preprint arXiv:0908.0333* (2009).

[23] E. Kiritsis and F. Nitti. “On massless 4D gravitons from asymptotically space–times”. In: *Nuclear Physics B* 772.1-2 (June 2007), pp. 67–102. ISSN: 0550-3213. DOI: 10.1016/j.nuclphysb.2007.02.024. URL: http://dx.doi.org/10.1016/j.nuclphysb.2007.02.024.

[24] Falk Bruckmann, Gergely Endrődi, and Tamas G Kovacs. “Inverse magnetic catalysis and the Polyakov loop”. In: *Journal of High Energy Physics* 2013.4 (2013), pp. 1–23.